

Petascale, Adaptive Computational Fluid Dynamics

Kenneth E. Jansen, Onkar Sahni, Min Zhou, Mark S. Shephard, Christopher Carothers, and Assad Oberai



Scientific Computation Research Center
Rensselaer Polytechnic Institute

Department of Mechanical, Aerospace and Nuclear Engineering

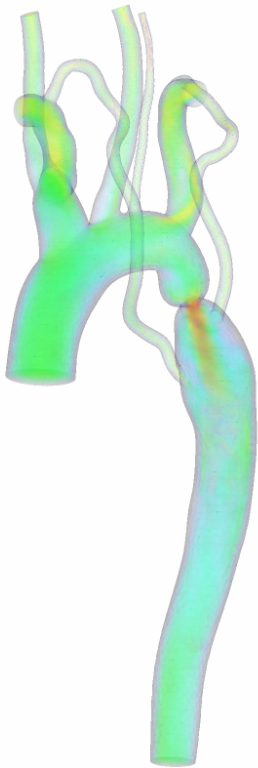
Outline

- Background and Motivation
- Computational Approach
- Current Scaling Results
- Adaptivity Approach
- Applications

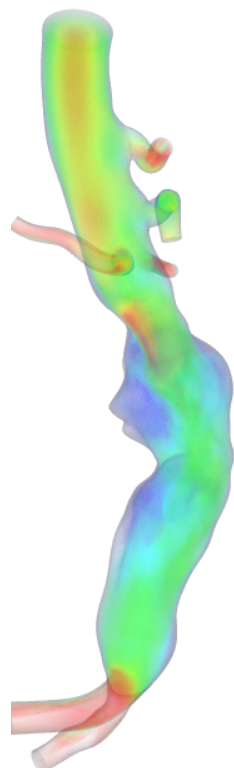
Flow Applications of Interest

Cardiovascular flows
(e.g., virtual surgical planning)

Human
coarctation

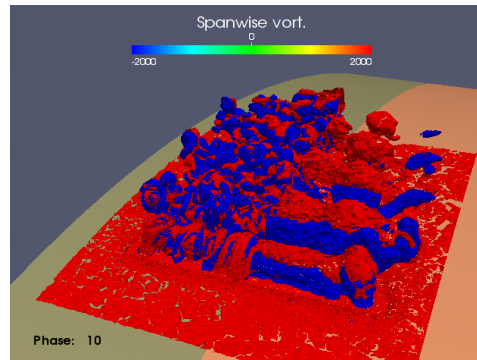


Abdominal aortic
aneurysm (AAA)

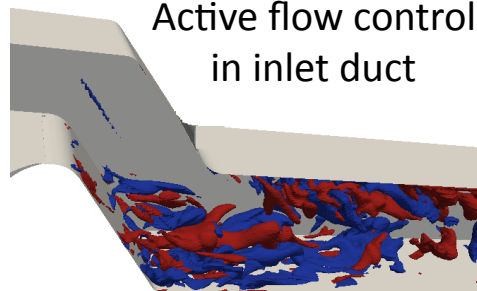


Aerodynamic flows
(e.g., aero “shaping”)

Active flow control
via synthetic jets on wings

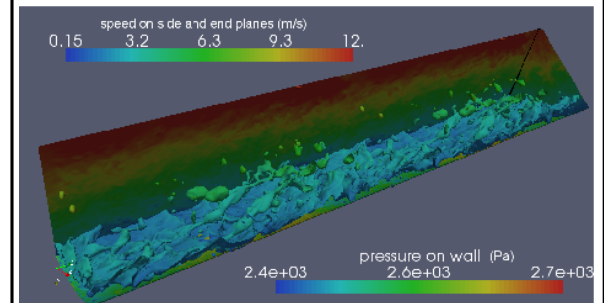


Active flow control
in inlet duct



Two-phase flows
(e.g., burnout prediction)

Two-phase annular flow

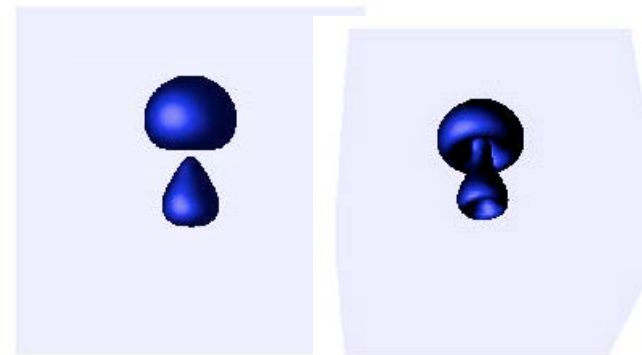
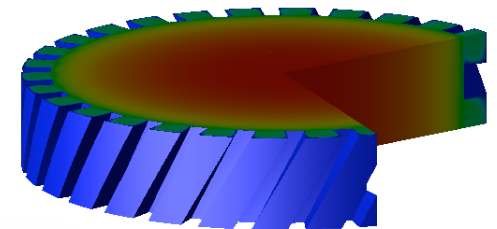
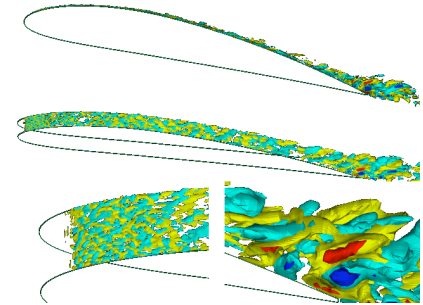


Plunging liquid jet



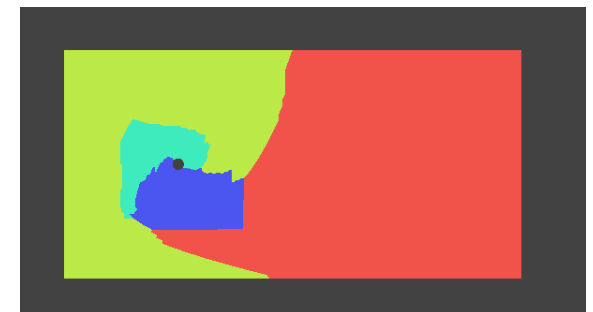
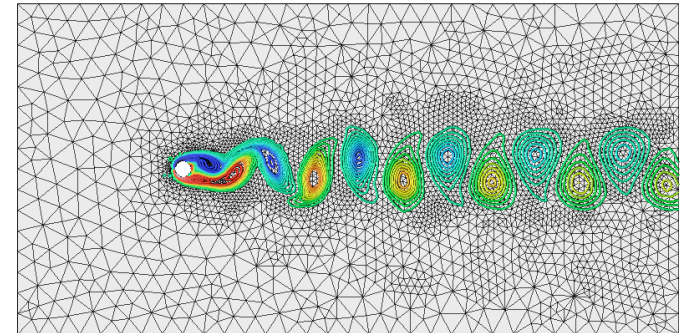
PHASTA Models

- Compressible or Incompressible
- Turbulence
 - Direct Numerical Simulation (DNS)
 - Large-Eddy Simulation (LES)
 - Reynolds-Averaged Navier-Stokes (RANSS)
 - Detached Eddy Simulation (DES) and other hybrid models
- History
 - Stanford (ENSA)
 - Euler 1985, Laminar NS 1988,
 - RANS 1991
 - CTR (Stanford-Ames)
 - Parallel LES 1994
 - RPI (ENSA evolves to PHASTA)
 - Parallel DES 2000,
 - Adaptivity 2002
 - Level set multiphase 2003
 - Parallel adaptivity 2006



PHASTA Flow Solver

- Stability with Accuracy
 - Hierarchic spatial basis (currently $p < 4$) $O(h^{p+1})$
 - Stabilized finite element method
 - Combined, yield accurate, well controlled, stabilization
 - Time integration: explicit (4th order RK) and implicit (2nd order generalized alpha method).
- Adaptivity
 - Grid matches physical scale
 - Anisotropic and transient
- Parallel
 - Excellent scaling to 160k processors on ANL Intrepid



Parallel Approach – NS Flow Solver

- Implicit non-linear FEM solver with two phases of computation:

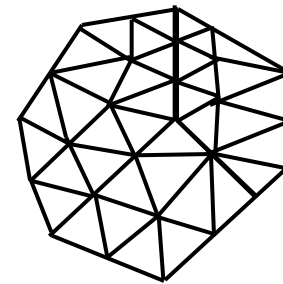
- **Equation formation** (*Eqn. form.*) – depends on *elements*

PDE/strong form – $\mathcal{L}Y = \mathcal{P}$

Weak form – $\int_{\Omega} (\cdot) d\Omega + \int_{\Gamma} (\cdot) d\Gamma$

Quadrature – $\boxed{\sum^{vol} (\cdot) + \sum^{bdy} (\cdot)}$

Assembly – $Ax = b$



- **Equation solution** (*Eqn. sol.*) – depends on *degrees-of-freedom (dofs)*:

Iterative solver

$Ax = b$

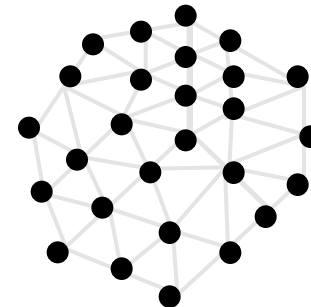
$p = b$

while

$q = Ap$

Orthonormalize q

...



Current Approach - Parallelization

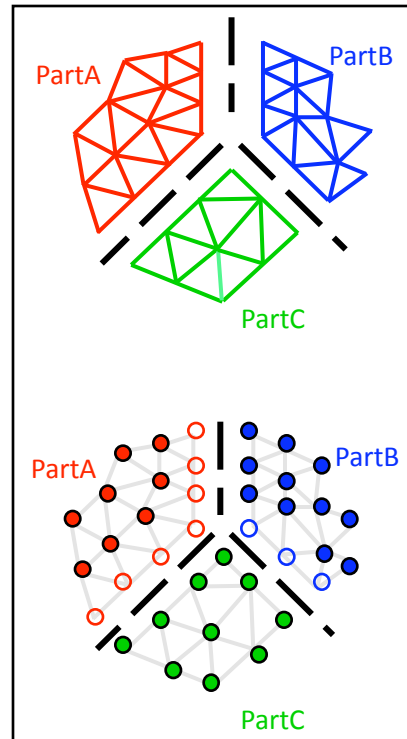
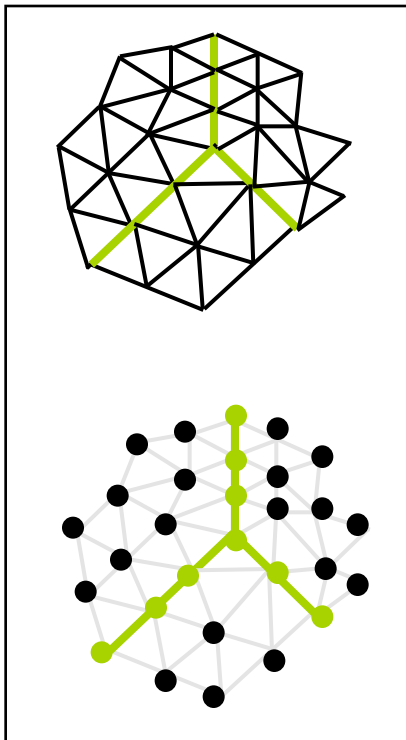
- Parallel strategy:
 - Both compute stages operate off the same mesh partition
 - Partition defines inter-part relations (part-to-part comm.)

Eqn. form.

$$\mathbf{Ax} = \mathbf{b}$$

Eqn. sol.

$$\mathbf{Ax} = \mathbf{b}$$



Locally, *incomplete* values
(in \mathbf{b} , \mathbf{A} , \mathbf{q} , etc.) for shared *dofs*.

Apply communications to *complete*
values/entries (in \mathbf{b} , \mathbf{q} only)

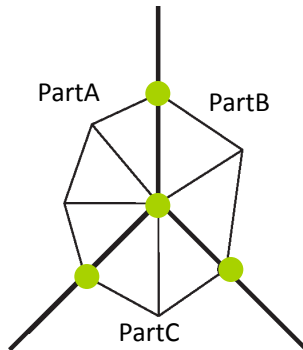
\mathbf{b} during Eqn. form.

\mathbf{q} during Eqn. sol.

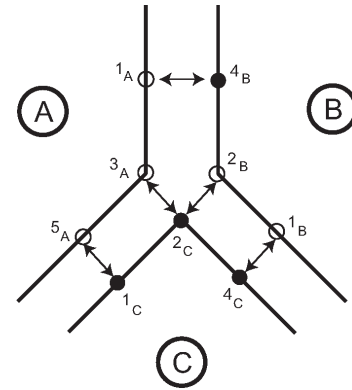
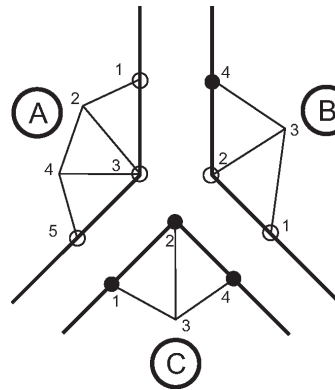
Current Approach – Parallelization

- Communications to *complete* values/entries and norms:

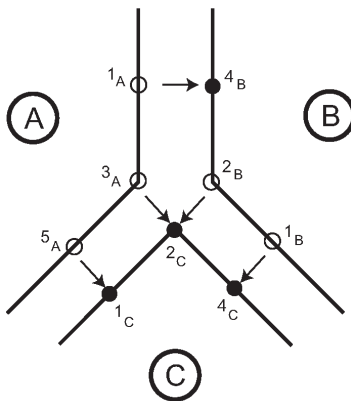
dofs are shared between parts



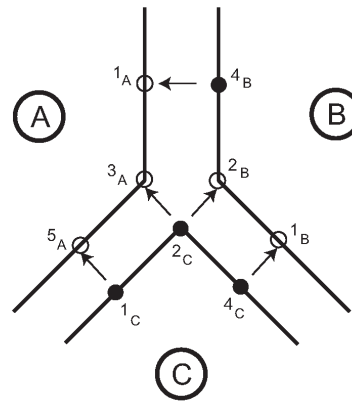
*control relationship between images
(solid dots indicate owner images)*



values accumulated on owners



values updated on to non-owners



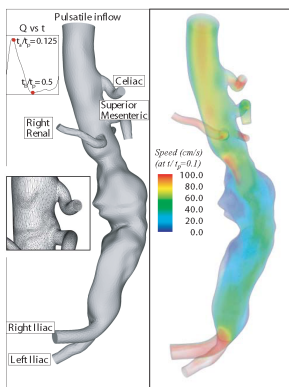
complete b

complete q
(for on-part $q=Ap$)

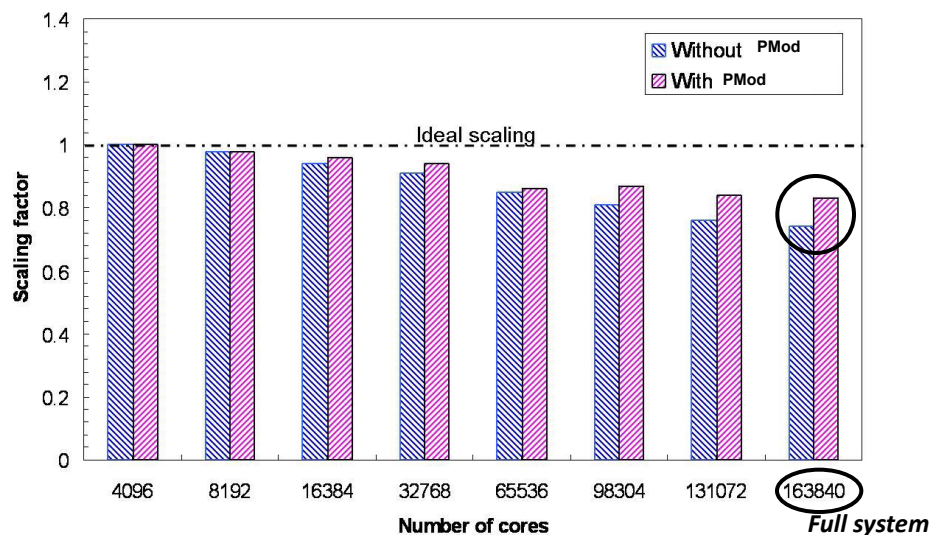
on-part norm for q
and all-reduce
(use complete q)

Strong Scaling – 1B Mesh up to 160k Cores

- AAA 1B elements: **effective partitioning** at extreme scale with and without partition modification (PMod)



1.07B elements mesh (Intrepid:IBM BG/P)	
num. of core	avg. elem./core
4,096 (base, 1 rack)	261,600
8,192; 16,384; 32,768	(see graph)
65,536 (16 racks)	16,350
98,304 (24 racks)	10,900
131,072 (32 racks)	8,175
163,840 (all 40 racks)	6,540



without PMod

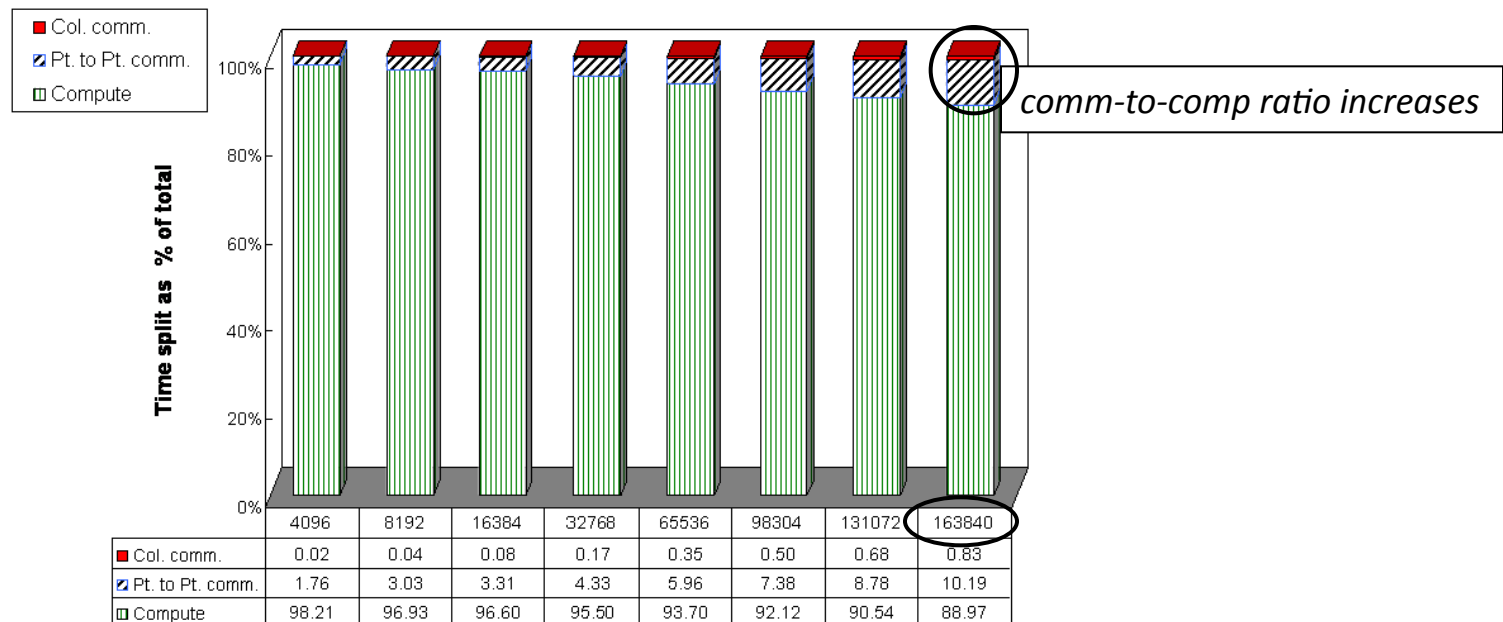
Eqn. form.	
time	s-factor
388.68	1
24.59	0.99
16.42	0.99
12.37	0.98
10.27	0.95
Eqn. soln.	
time	s-factor
456.24	1
33.70	0.85
23.56	0.81
18.65	0.76
15.34	0.74
Total	
time	s-factor
844.92	1
58.29	0.91
39.98	0.88
31.02	0.85
25.61	0.82

with PMod

Eqn. form.	
time	s-factor
388.90	1
25.48	0.95
17.12	0.95
12.79	0.95
10.46	0.93
Eqn. soln.	
time	s-factor
455.48	1
33.17	0.86
21.94	0.87
16.89	0.84
13.66	0.83
Total	
time	s-factor
844.38	1
58.65	0.91
39.06	0.90
29.68	0.89
24.12	0.88

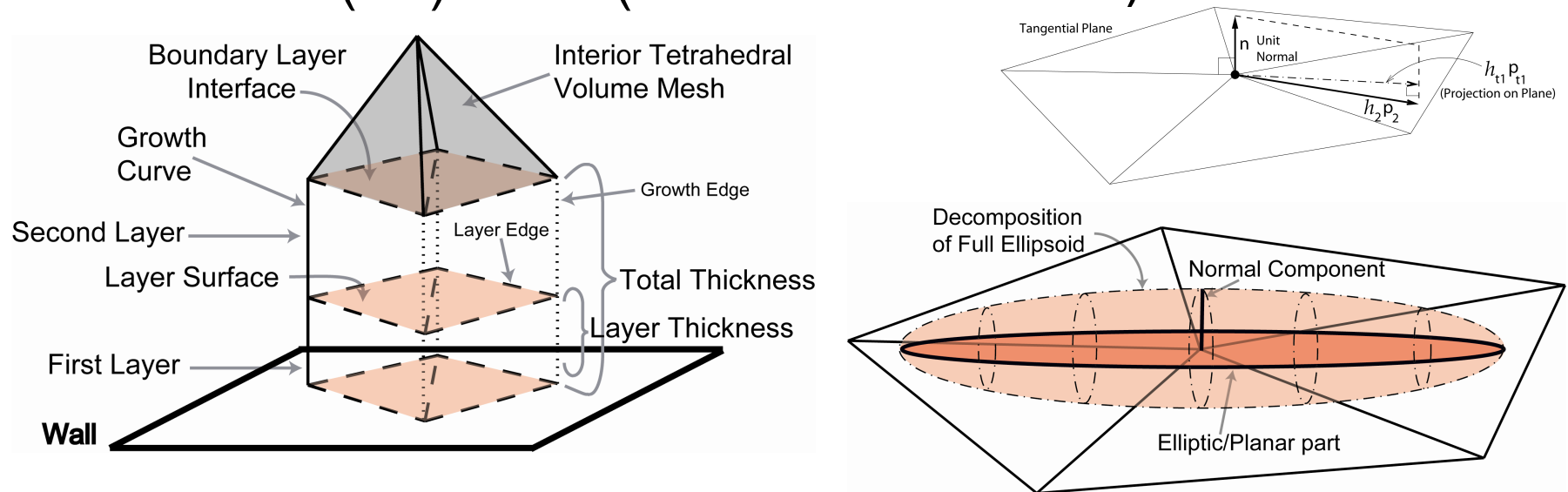
Strong Scaling – 1B Mesh up to 160k Cores

1.07B elements mesh (Intrepid:IBM BG/P)		$t_{tot} (=t_{comm}+t_{comp})$	t_{comm}	t_{comp}	
num. of cores	avg. elem./core	absolute	% of t_{tot}	% of t_{tot}	s-factor
4,096 (base, 1 rack)	261,600	844.38	1.79%	98.21%	1
8,192 (2 racks)	130,800	427.33	3.07%	96.93%	1.00
16,384 (4 racks)	65,400	217.05	3.40%	96.60%	0.99
32,768 (8 racks)	32,700	109.87	4.50%	95.50%	0.99
65,536 (16 racks)	16,350	58.65	6.30%	93.70%	0.94
98,304 (24 racks)	10,900	39.06	7.88%	92.12%	0.96
131,072 (32 racks)	8,175	29.68	9.46%	90.54%	0.96
163,840 (all 40 racks)	6,540	24.12	11.03%	88.97%	0.97

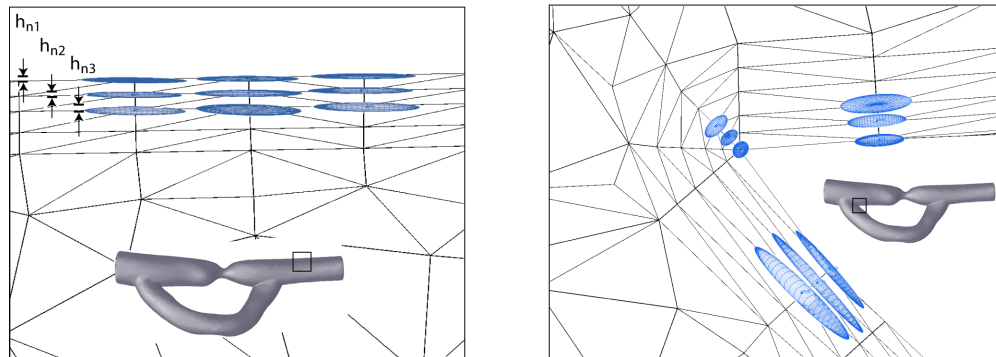


Boundary Layer Mesh Adaptation

- Decompose layers into layer surfaces (2D) and a thickness (1D) mesh (O. Sahni Ph.D work).

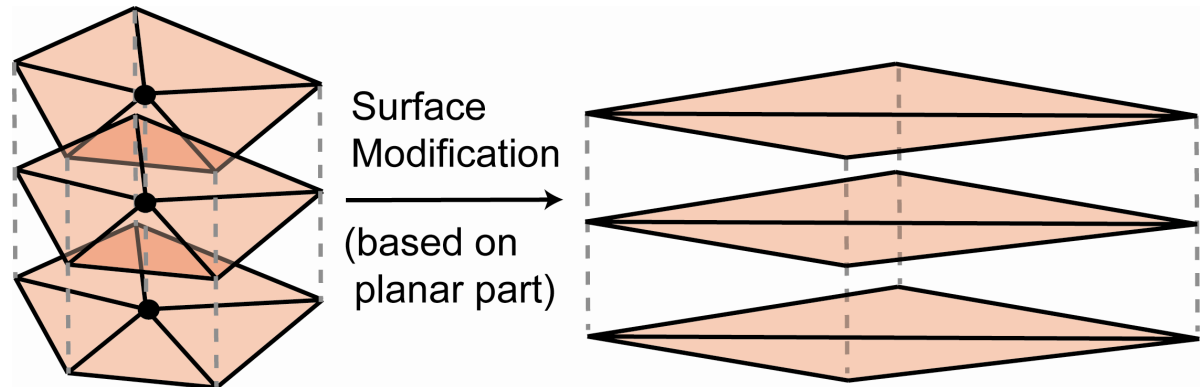


- A typical example:

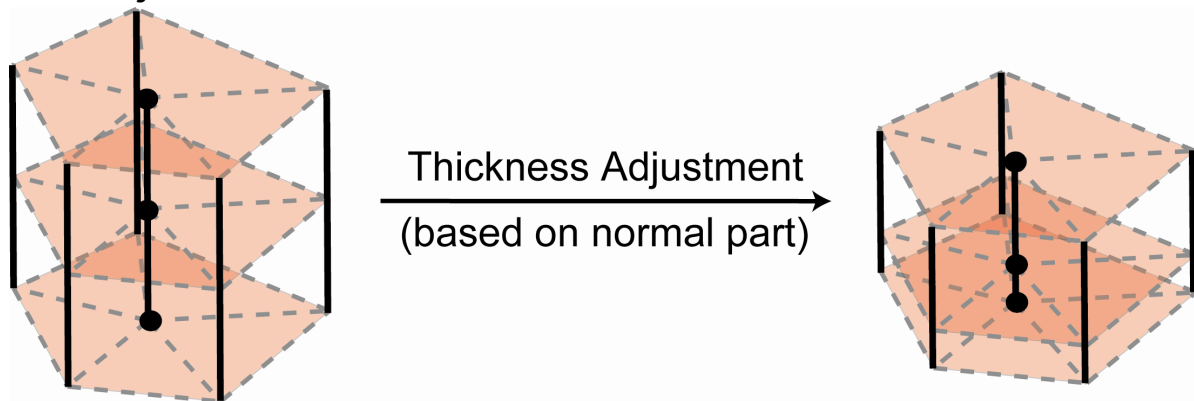


Two Steps of Layered-Mesh Modification

- Mesh modification procedure for layered part is divided into two steps:
 - Layer surface mesh modification



- Layer thickness mesh adjustment



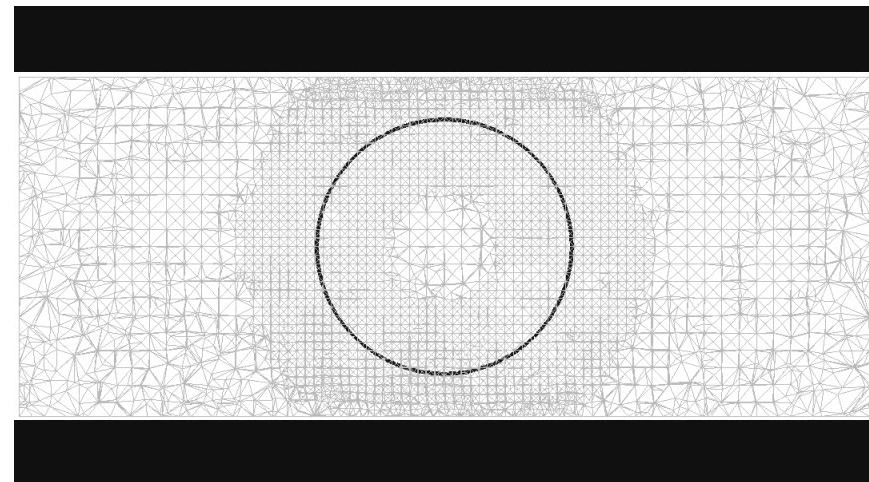
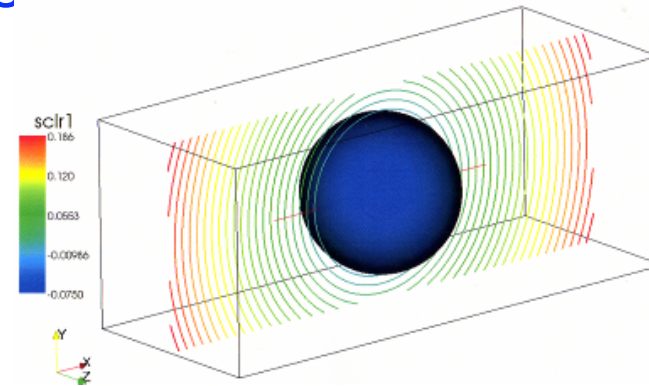
Level Set Two Phase Example

(Rodriguez)

- Sphere advected through periodic domain

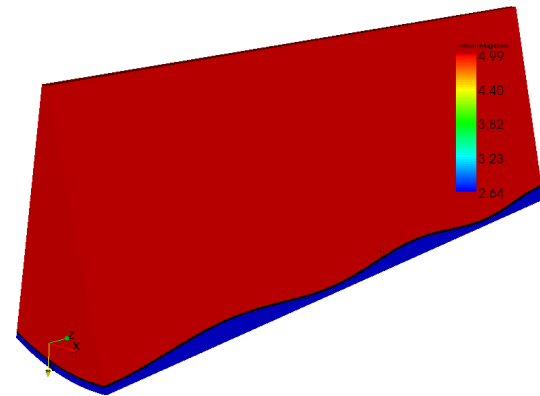
$$Size = \begin{cases} 0.005 & , \quad |\phi| < \varepsilon \\ \frac{(0.005 + 0.02)}{2} & , \quad \varepsilon < |\phi| < 3\varepsilon \\ 0.02 & , \quad |\phi| > 3\varepsilon \end{cases}$$

- Scalar equation advects to maintain distance to interface
- Viscosity and density determined from scalar



Annular Flow Simulation (Rodriguez)

- Simulate annular flow run similar to RISO run #602 ⁽¹⁾
 - Steam/water @ 70bar
 - 0.01m radius vertical tube
 - 30% exit quality, $G_{IN} = 500 \text{ kg/s-m}^2$
 - $Re_\tau \sim 800$
 - $\delta_m = 0.94 \text{ mm}$
- Model
 - 30° wedge
 - $L=0.025\text{m}$
- Boundary Conditions
 - Axial and circumferential: periodic
 - Radial: symmetry (inside), wall (outside)
 - Applied pressure gradient from RISO test



Phase Interface Evolution (Rodriguez)

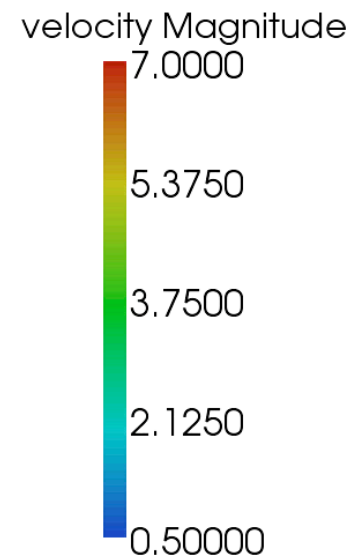
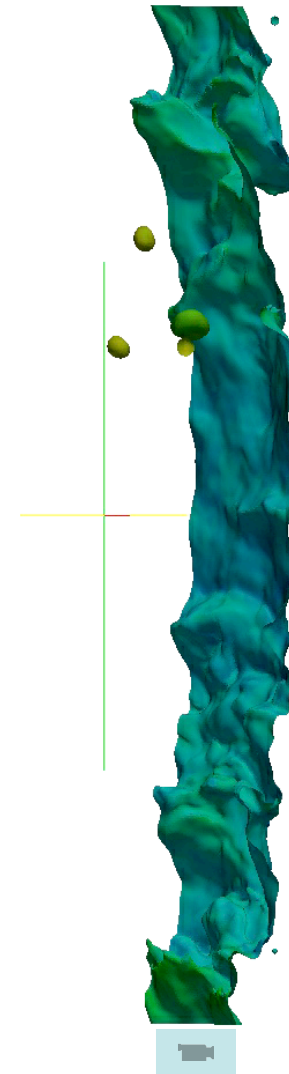
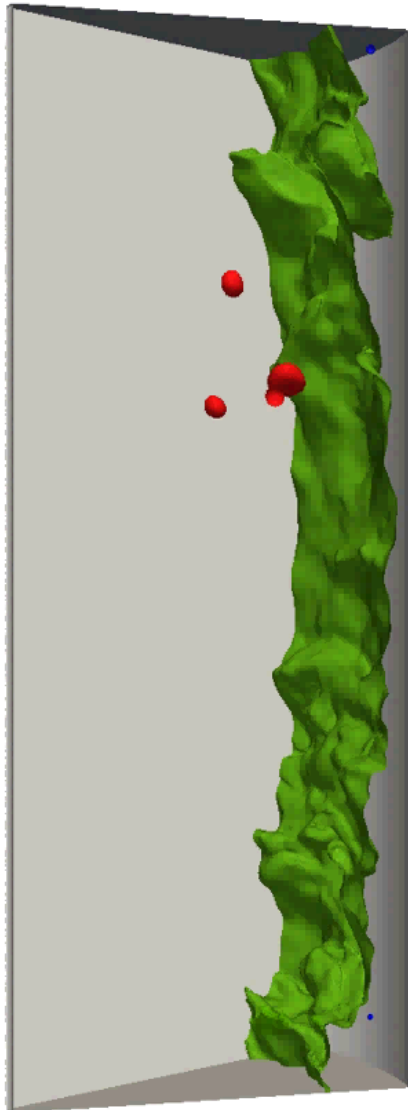
Time: 54.6863 msec

LEGEND

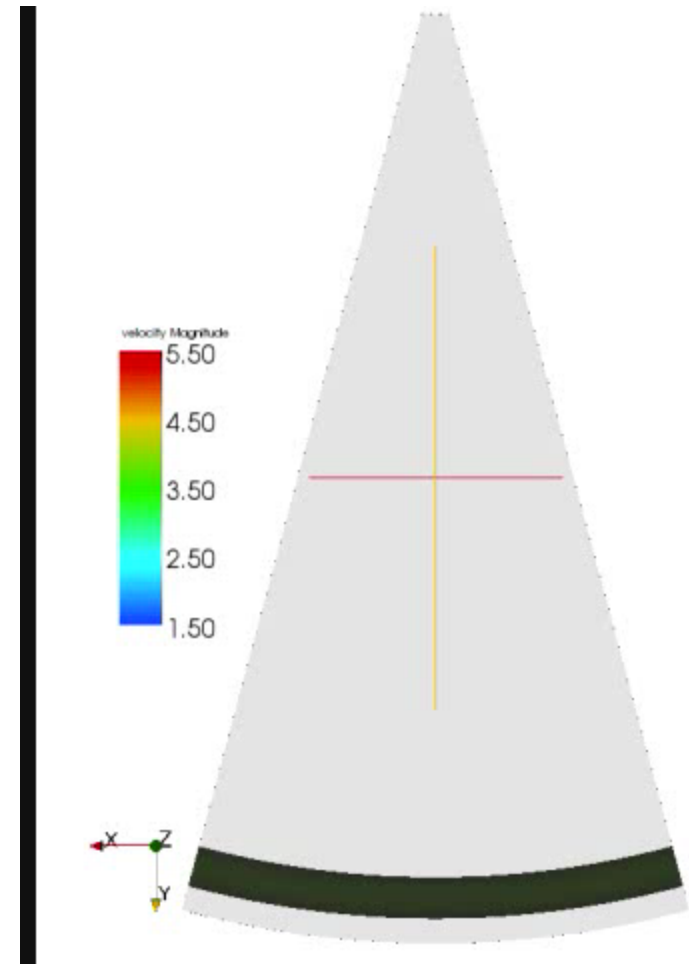
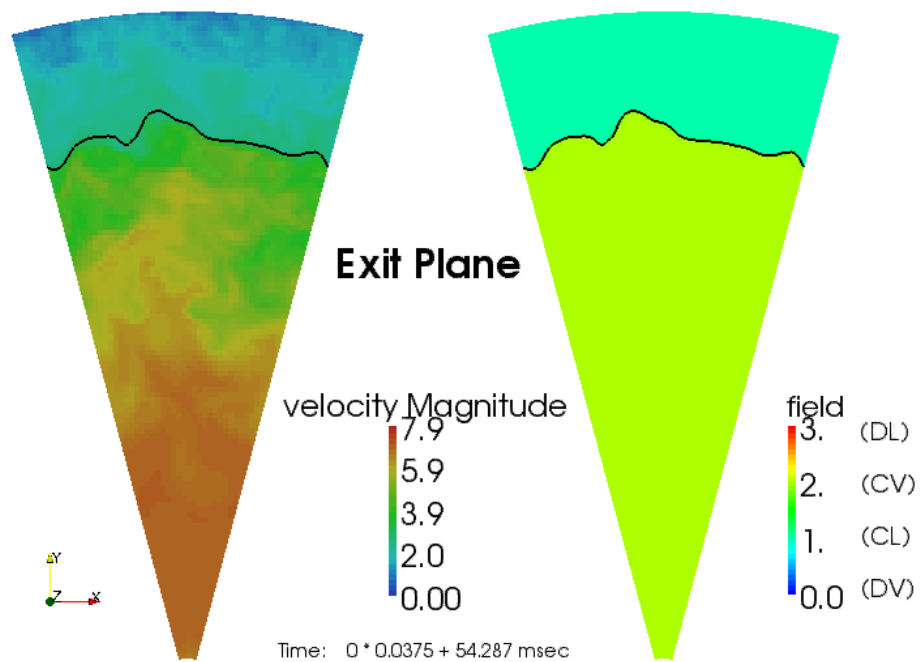
Bubble

Droplet

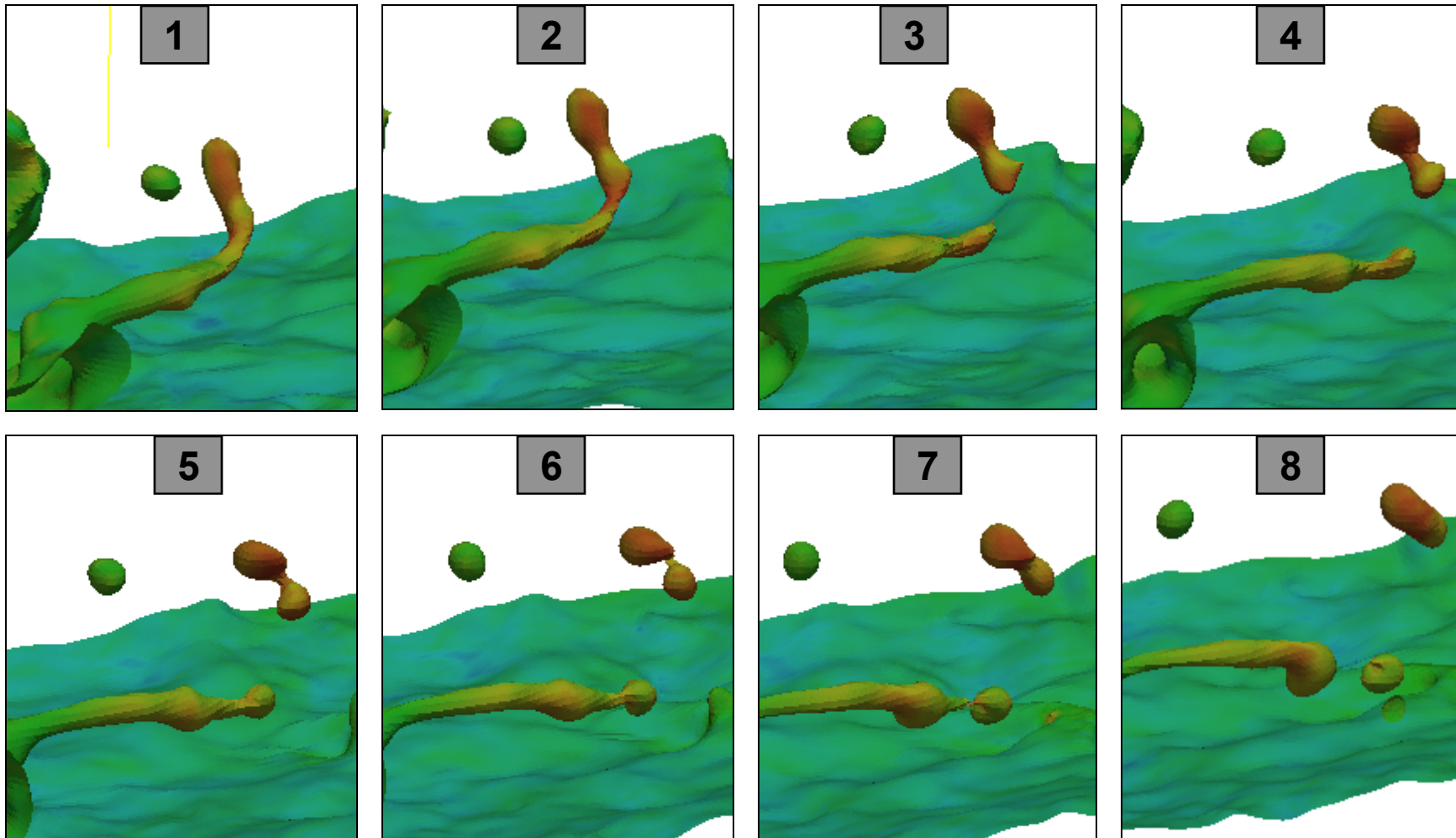
Liquid Film



Phase Interface Evolution (Rodriguez)



Droplet Entrainment (Rodriguez)

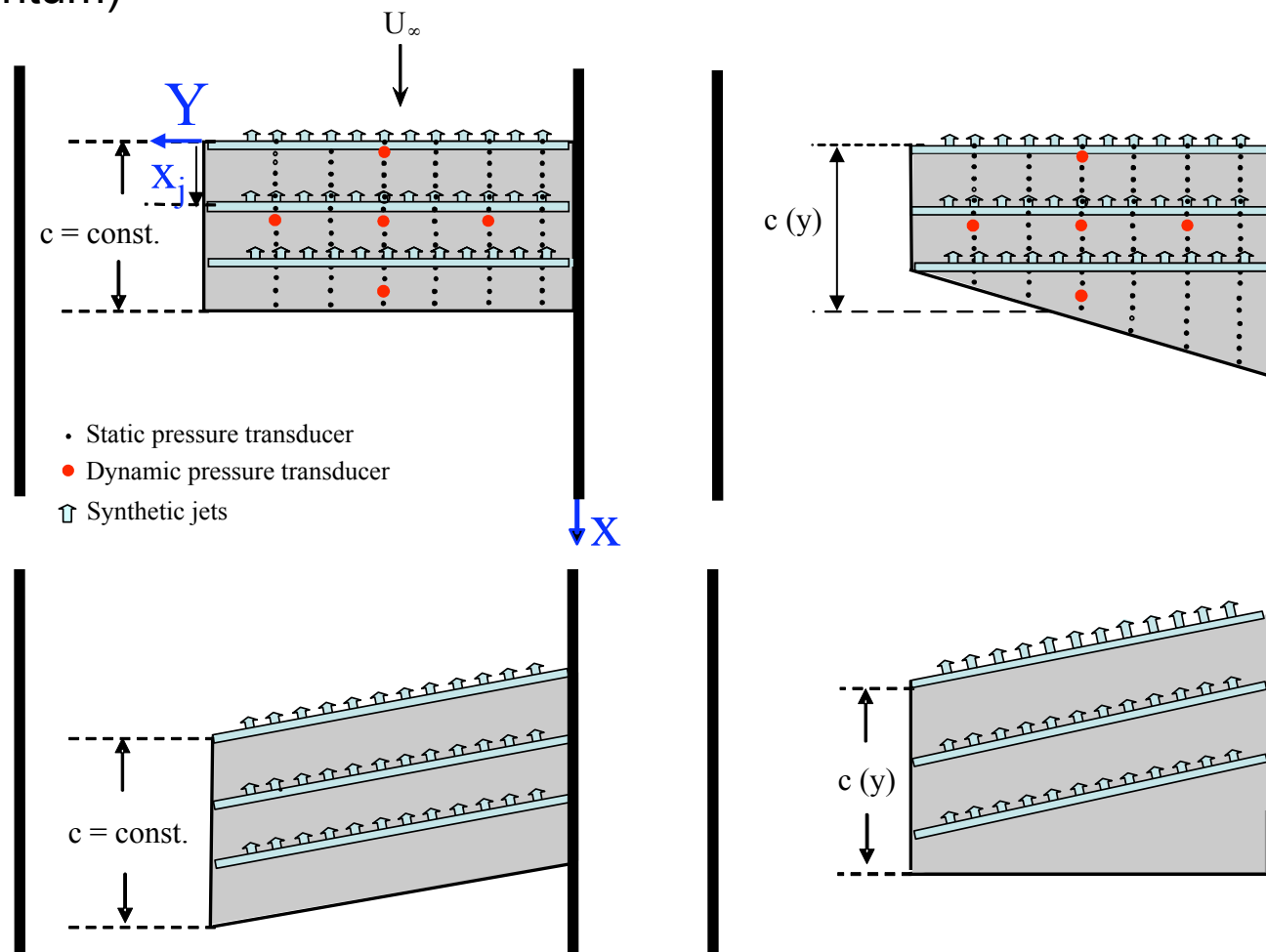


Multiphase Simulation: Scientific/ Engineering Value

- Simulations are being averaged to validate against RISO experimental data: void profiles, field flow rates, wave frequencies.
- Once validated, they will be used to develop closure models for phase field models
 - E.g. 4 field models evolve distinct Navier-Stokes p.d.e.s for:
 - Continuous liquid
 - Continuous vapor
 - Discontinuous liquid (drops)
 - Discontinuous vapor (bubbles)
 - Conditional sampling of our simulation on each of these 4 fields allows turbulence statistics and time-averaged phase fractions to be determined.
- Fundamental physics gleaned from transient fields guides modeling process.
- DOE NERI project couples PHASTA Multiphase to phase field models (NPHASE) to model Gen IV reactor accidents.

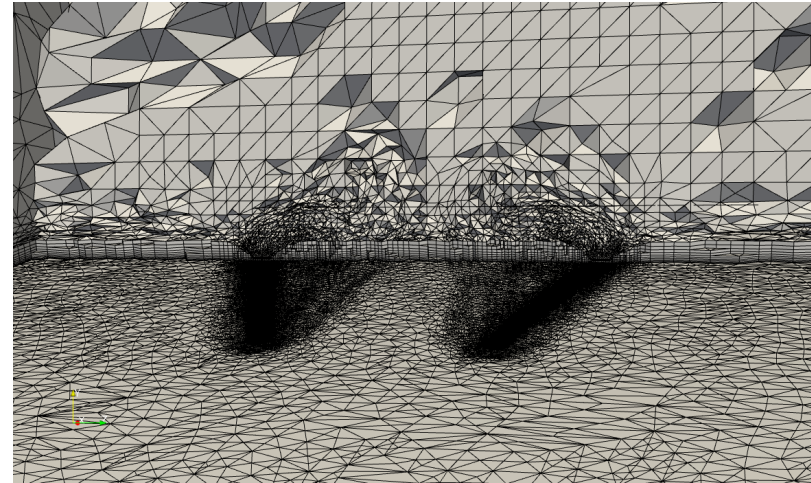
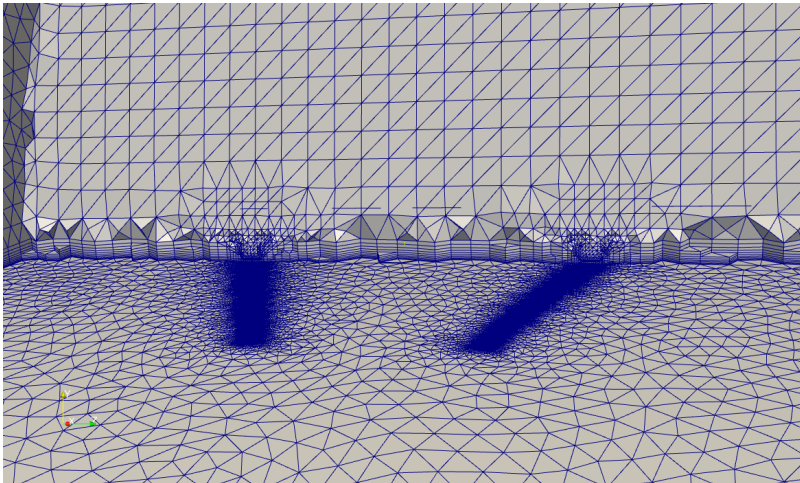
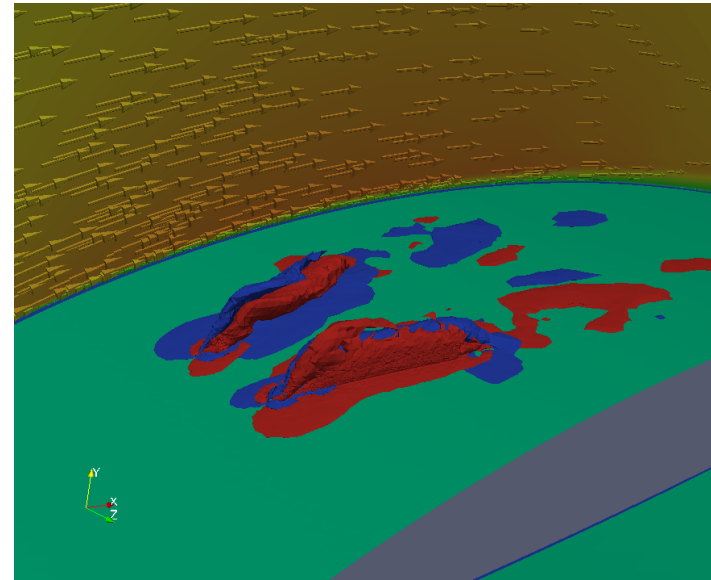
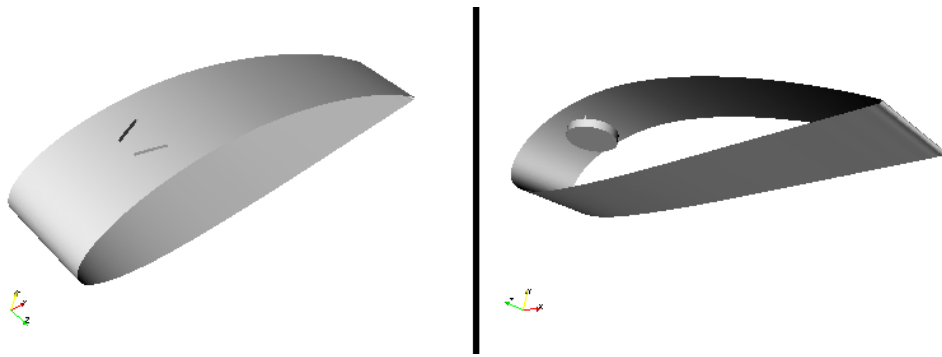
Flow Control using Synthetic Jets: AFOSR

Synthetic jets combine a piezoelectric disk, a resonant cavity, and a slit or hole to produce an unsteady jet (zero net mass but significant net momentum)

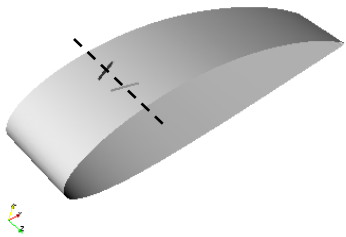


Mesh Adaptivity for Synthetic Jets(O. Sahni)

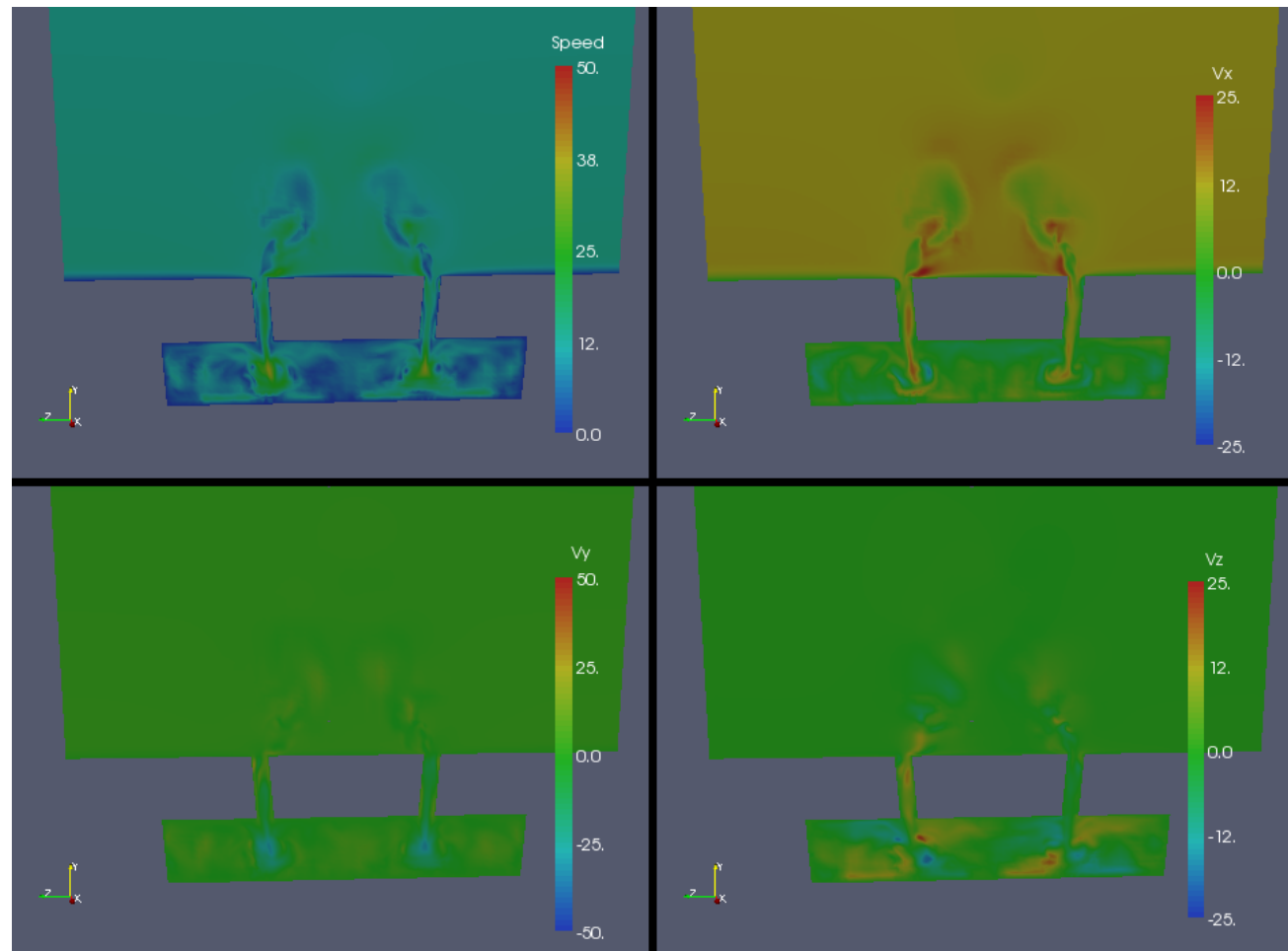
$f_{act} = 2,300\text{Hz}$
 $\alpha = 0^\circ$
 $Re \sim O(100,000)$



Synthetic Jets for 0° AOA (CFD)



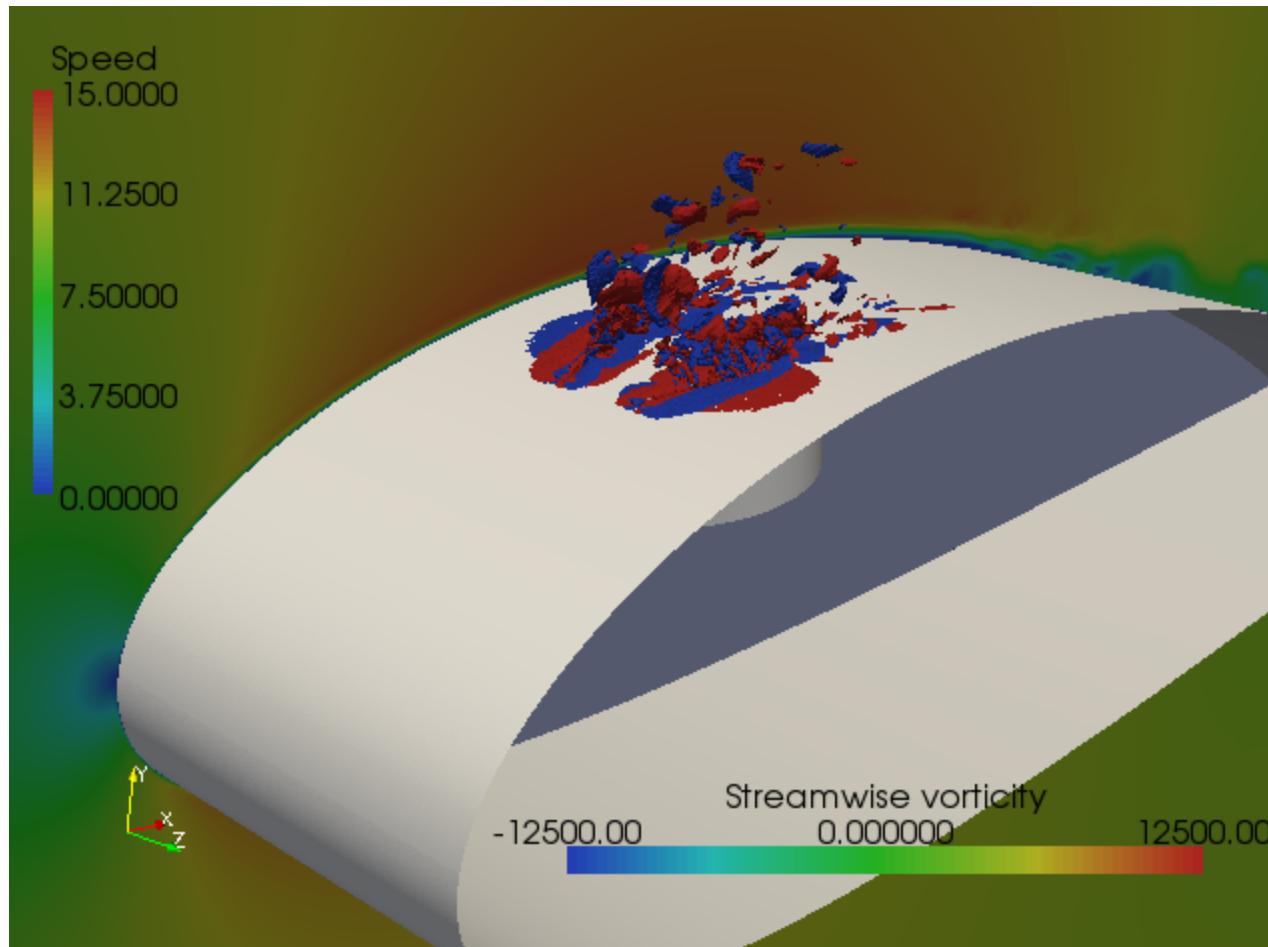
$C_\mu = 7.25 \times 10^{-3}$
 $C_b = 3.2$
 $f_{act} = 2,300 \text{ Hz}$
 $f_{conv} = O(100 \text{ Hz})$
 $\alpha = 0^\circ$
 $Re = 100,000$



Structures rise 8-10 slit widths as in experiment

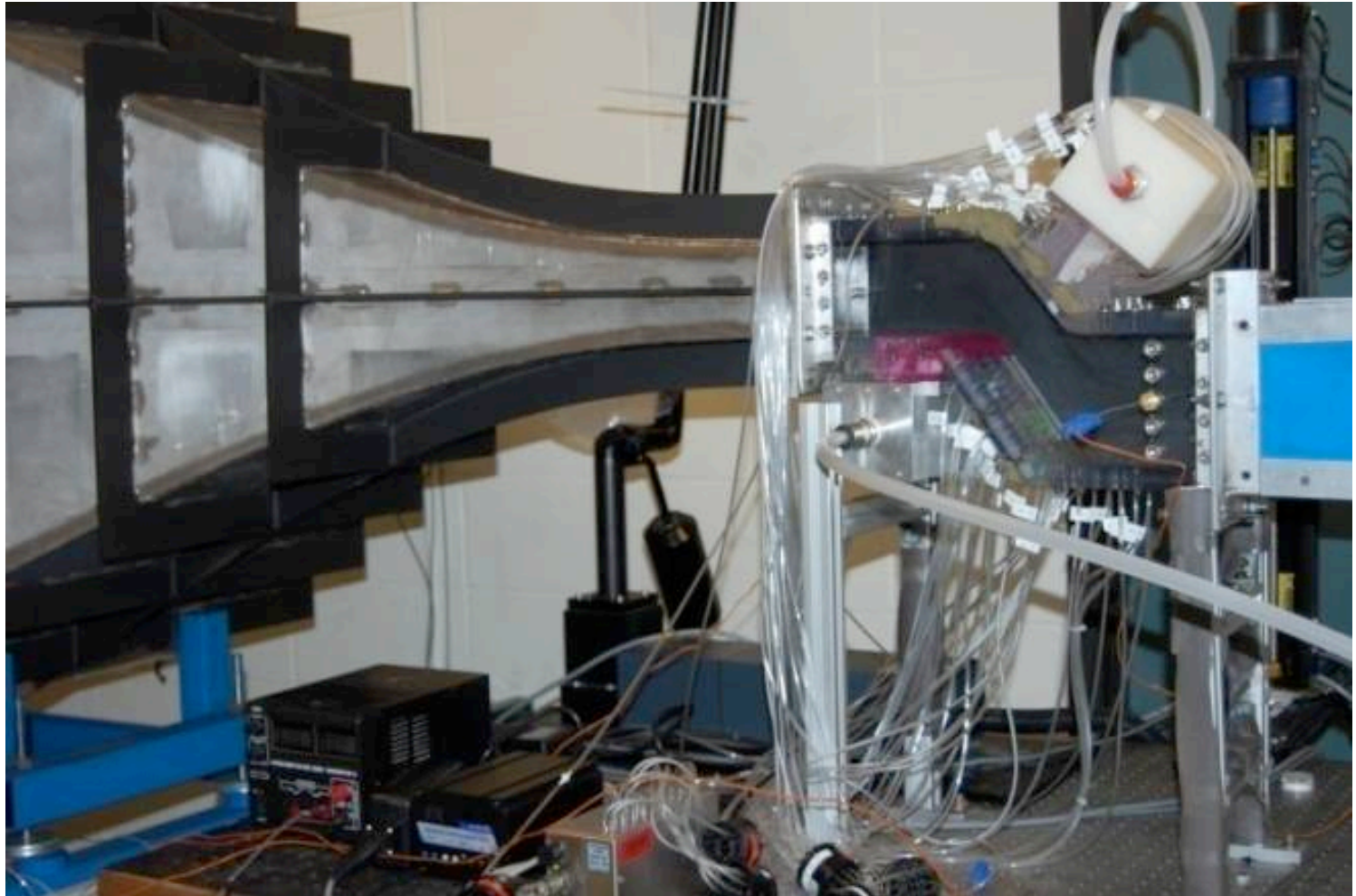
Synthetic Jets for 0° AOA (CFD)

$C_\mu = 7.25 \times 10^{-3}$
 $C_b = 3.2$
 $f_{act} = 2,300\text{Hz}$
 $f_{conv} = O(100\text{Hz})$
 $\alpha = 0^\circ$
 $Re = 100,000$



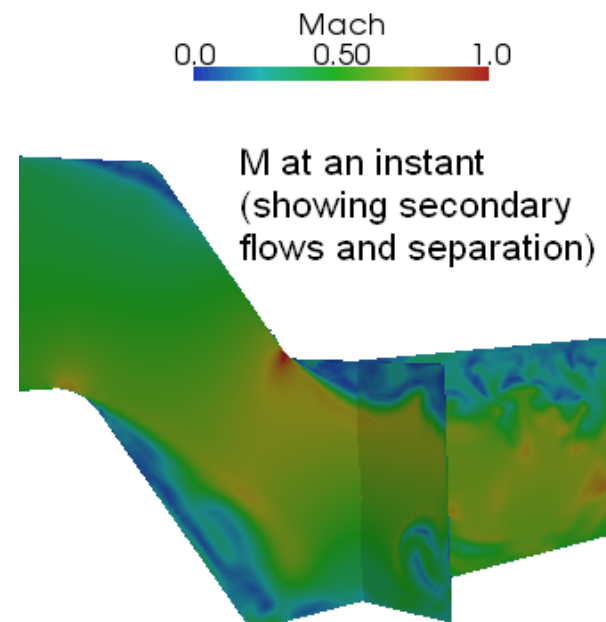
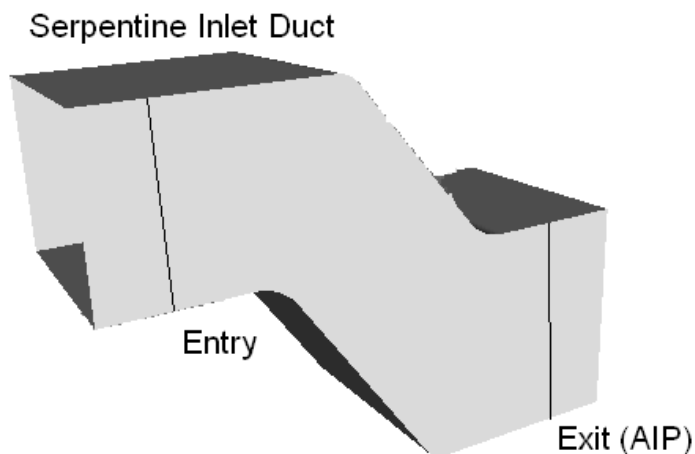
Jet flow structures persist $0.2c$ as in experiment.

Flow Control: Experiment/CFD/Controls w. Amitay & Wen



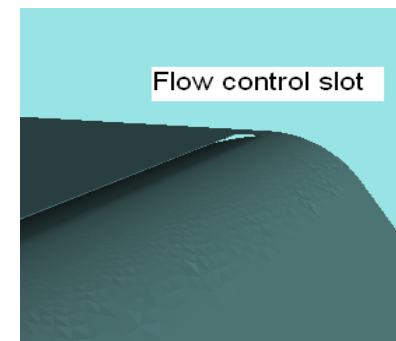
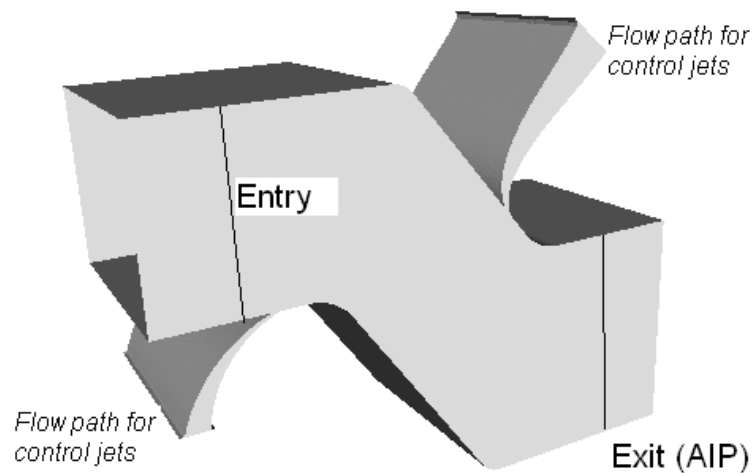
Flow in Serpentine Inlet Ducts

- Short inlet ducts with curvature are required for applications with constraints on packing and low-observability.
- Flow separation and secondary flows
- Pressure loss and distortion at the AIP:

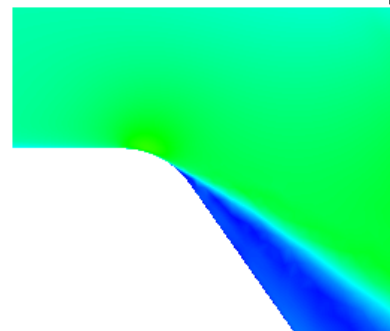


Active Flow Control (tangential blowing)

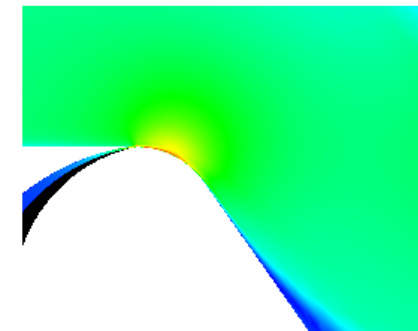
- Active flow control through tangential blowing (e.g., 0.8% of main flow):



Example of active flow control



Baseline flow (no flow control)

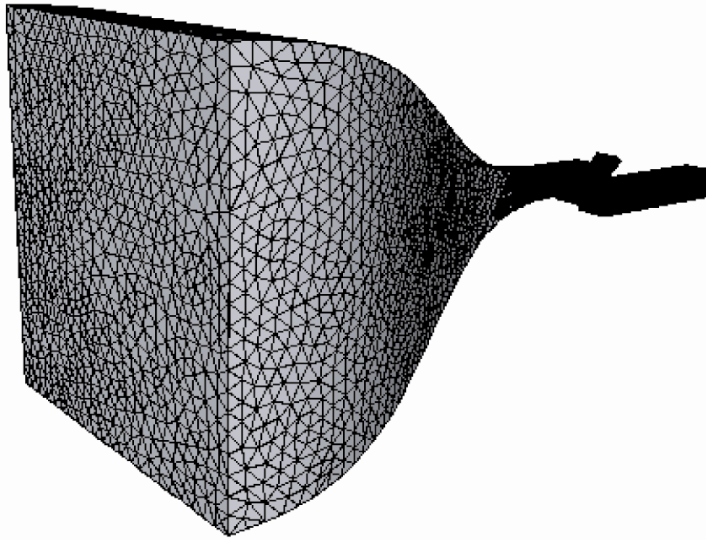


Active flow control
(tangential blowing)

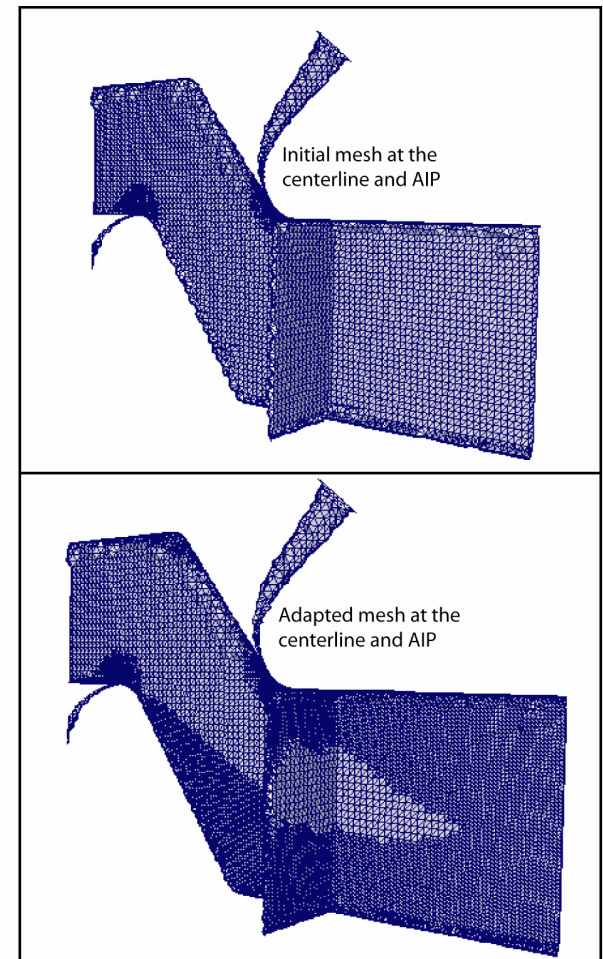
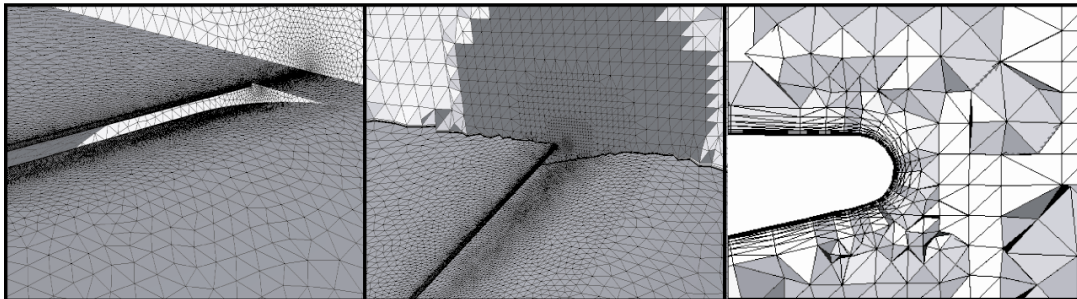
Adaptive Meshing for Inlet Duct

- Unstructured (boundary layer) mesh; initial mesh (M_{coarse}) $\sim 2.5\text{M}$ nodes, Adapted mesh (M_{fine}) $\sim 4\text{M}$ nodes

Surface mesh of the full domain

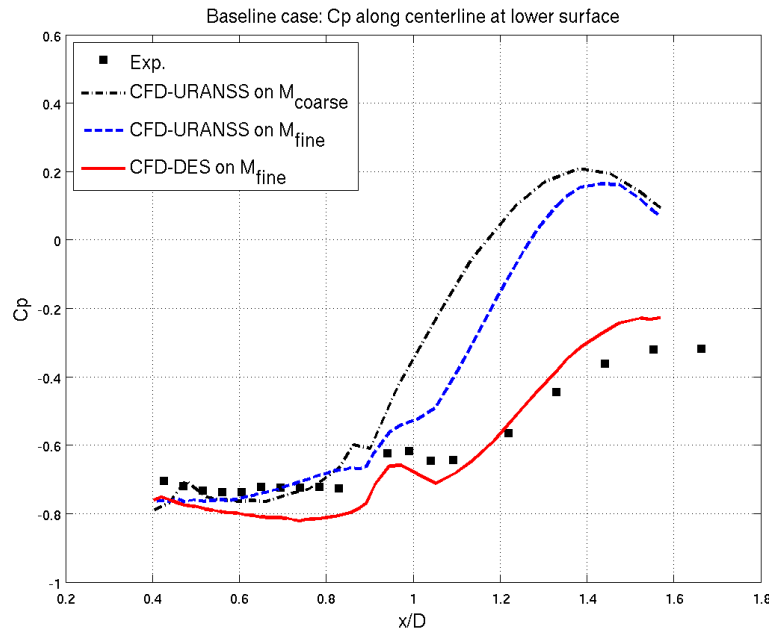


Surface and interior mesh faces near the lower flow control slot

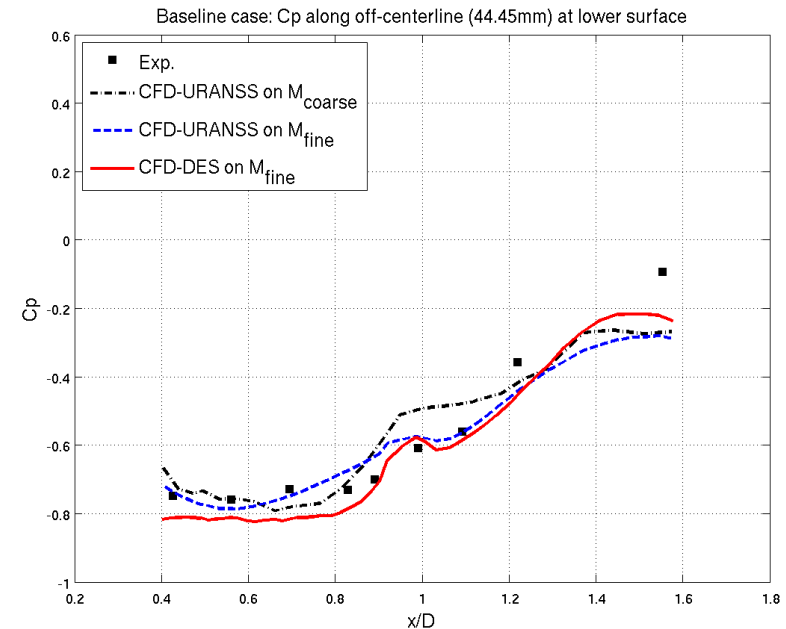


Baseline: Static Pressure Lower Wall (C_p)

- Centerline



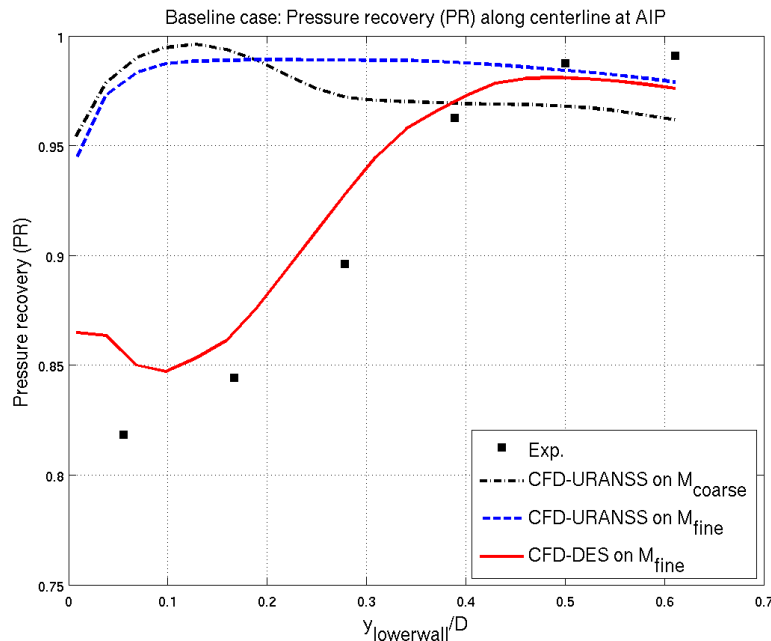
$\frac{1}{4}$ Span



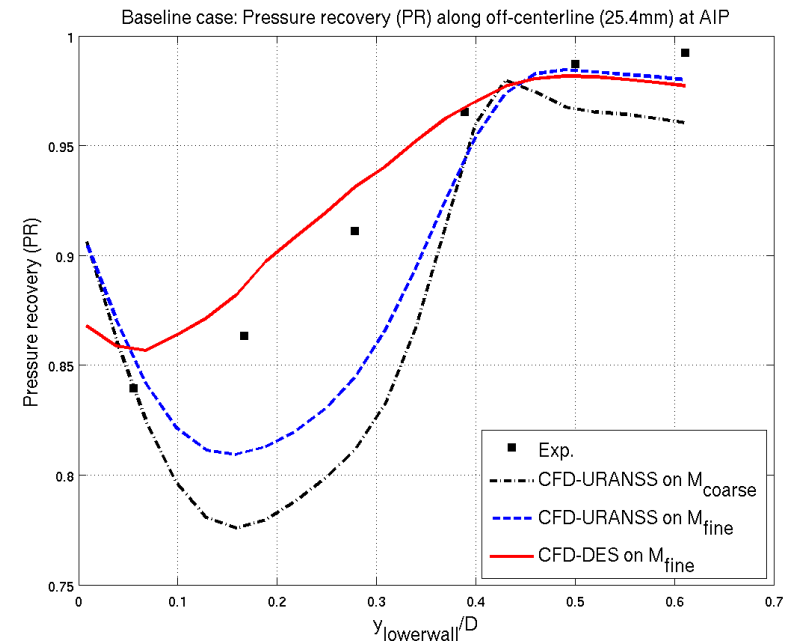
- DES predictions are in good agreement with the experimental measurements
- URANSS predictions on centerline are poor and do not improve with mesh refinement

Baseline: Total Pressure Distribution (PR)

- Centerline



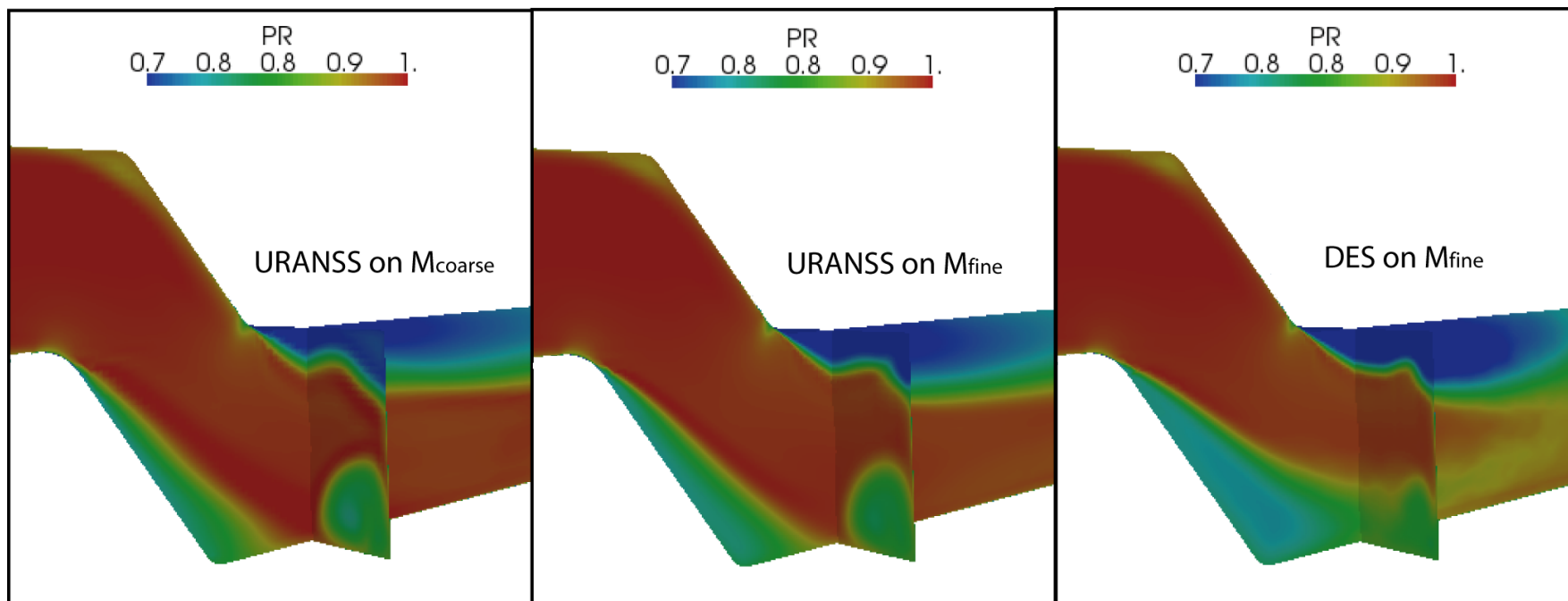
- $\frac{1}{4}$ Span



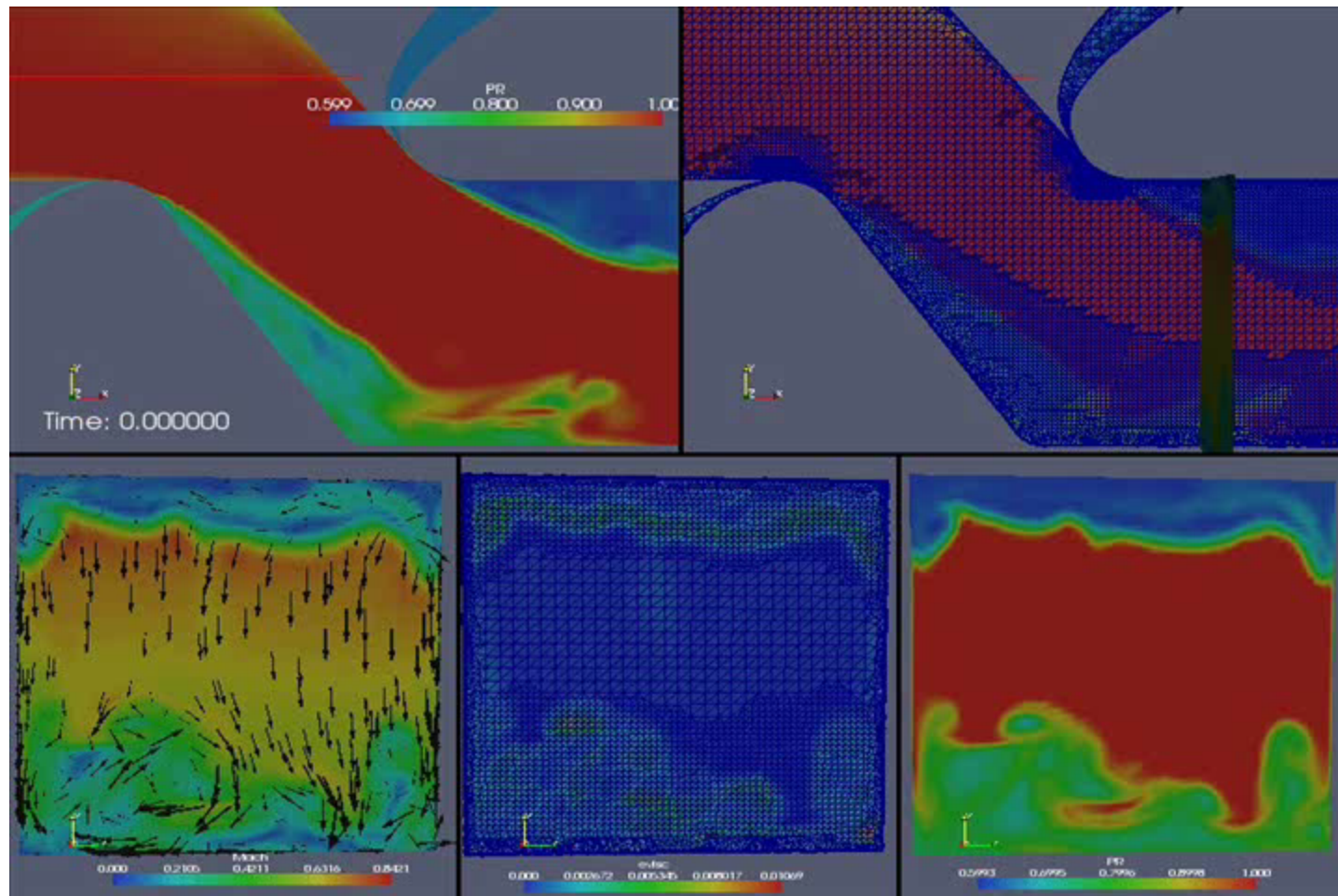
- Pressure recovery for baseline flow: as before, DES results are in better agreement than URANSS.

Baseline: Pressure Recovery Field

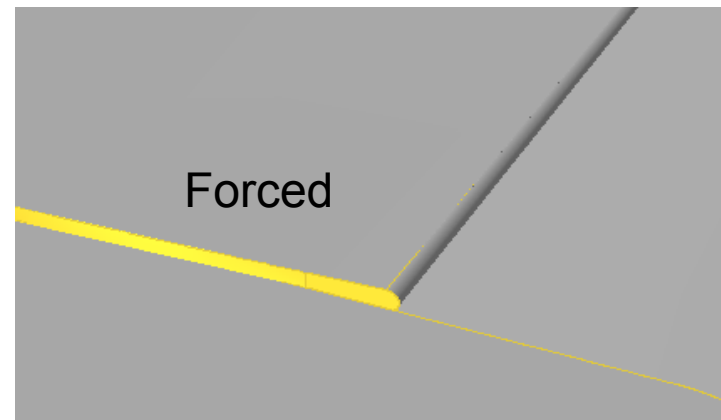
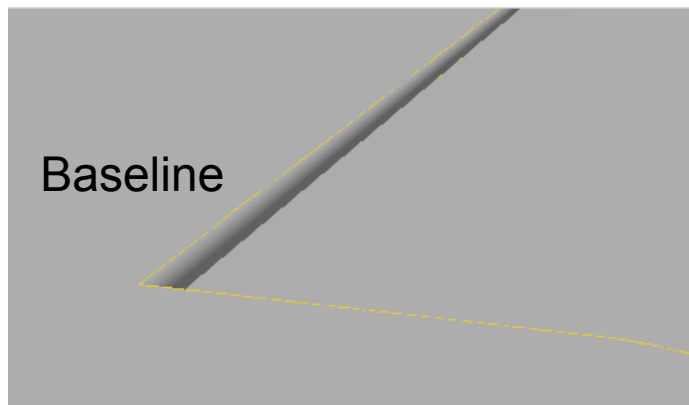
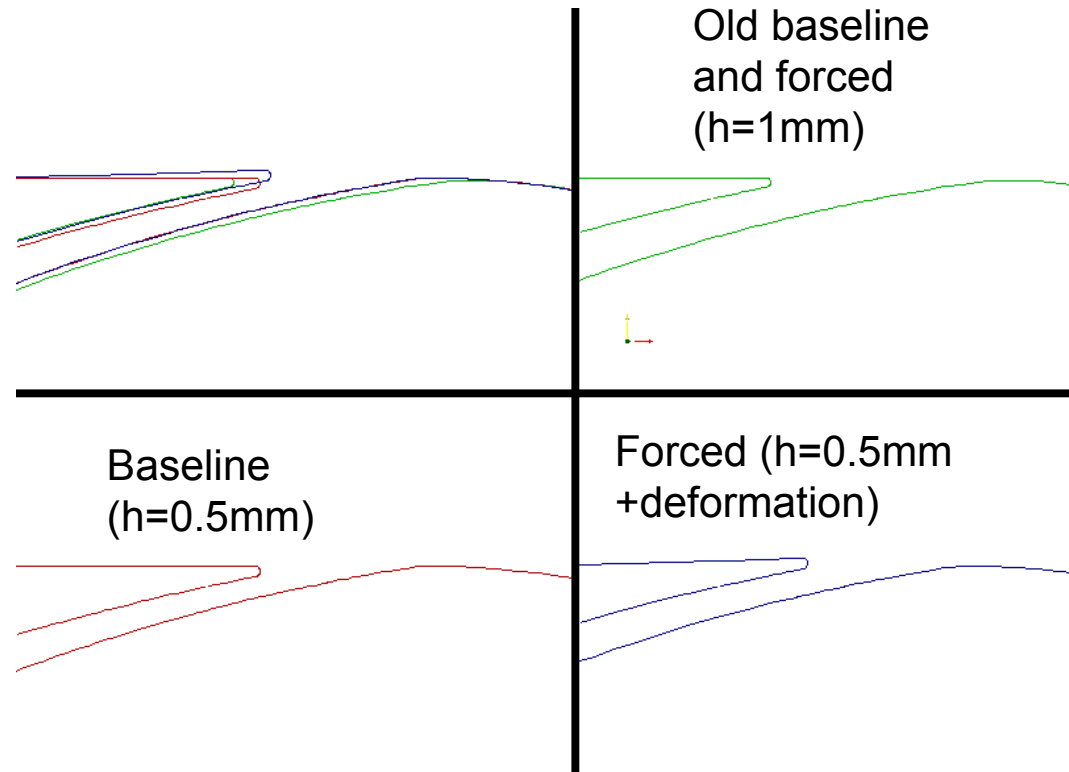
- Time averaged pressure recovery
- URANSS predicts large, stable vortices at lower corners that pull flow down at centerline
- Result: Incorrect high pressure values seen in C_p and PR for URANSS:



CFD: DES Results





New geometry



Flow Control Simulation: Scientific/ Engineering Value

- Simultaneous, precisely matched experiments is challenging, and requires iteration to validate CFD for flow control
- Once validated, simulations provide detailed field data to understand flow structures that are most effective for controlling the flow.
- Statistics from unsteady simulations may be helpful in developing improved RANSS models
- Open and closed loop controls are being integrated with the CFD to explore design of new flow control actuators and optimal sensor placement.
- Three active grants with matched experiments (Amitay); two of which have controls component (Wen).
- Future applications in wind turbines looks very promising and will require fluid-structure interactions.

Conclusions

- Complex geometry/physics=> Real world Apps
- Implicit solvers: Complexity  but n_{step} 
- Excellent scaling results
- Big Science AND FAST SCIENCE
- Adaptivity brings real geometry problems into reach of solution in a USEFUL time frame
- Multiphase simulation capable of modeling turbulent flow with mixture of steam and water
- Complex geometry of very small flow control devices being simulated and validated.

Acknowledgements

- Grants:
 - NSF grant OCI-0749152 under PetaApps program
 - DOE grant DE-FC02-06ER25769 under SciDAC program
- Computing systems and support:
 - ALCF at ANL (Intrepid system)
- Software components:
 - AcuSim Inc., Simmetrix Inc., Kitware Inc., Zoltan ...
- Special thanks to:
 - Ray Loy, Adam Todorski, Bob Walkup, Karen Devine, Chris Carothers, Charles Taylor, Tim Wickberg and Katherine Riley

Stabilized Finite Element Formulation

$$B(w_i, q; u_i, p) = 0$$

$$B(w_i, q; u_i, p) = \int_{\Omega} \{w_i (\dot{u}_i + u_j u_{i,j} - f_i) + w_{i,j} (-p \delta_{ij} + \tau_{ij}) - q_i u_i\} dx \\ + \int_{\Gamma_h} \{w_i (p \delta_{in} - \tau_{in}) + q u_n\} ds$$

Galerkin

$$+ \sum_{e=1}^{n_{el}} \int_{\bar{\Omega}_e} \{\tau_M (u_j w_{i,j} + q_i) \mathcal{L}_i + \tau_C w_{i,i} u_{j,j}\} dx$$

SUPG stabilization

$$+ \sum_{e=1}^{n_{el}} \int_{\bar{\Omega}_e} \{w_i \overset{\Delta}{u}_j u_{i,j} + \bar{\tau} \overset{\Delta}{u}_j w_{i,j} \overset{\Delta}{u}_k u_{i,k}\} dx$$

Restores conservation

where

$$\mathcal{L}_i = \dot{u}_i + u_j u_{i,j} + p_i - \tau_{ij,j} - f_i,$$

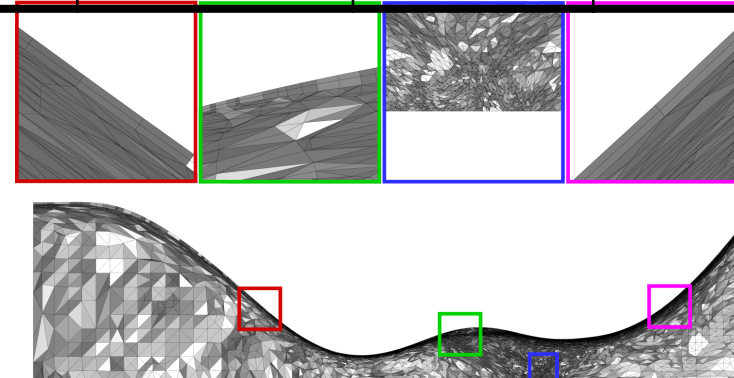
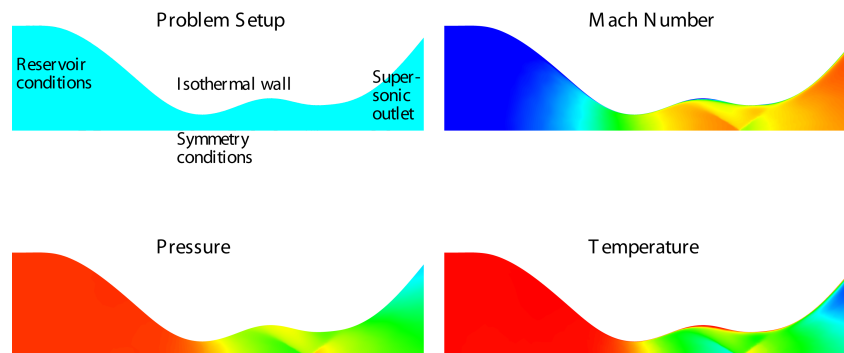
$$\overset{\Delta}{u}_i = -\tau_M \mathcal{L}_i$$

Compressible Implicit Flow Solver – Compresses Time

- Strong scalability results for double-throat nozzle (approx. 1.5M elems.):

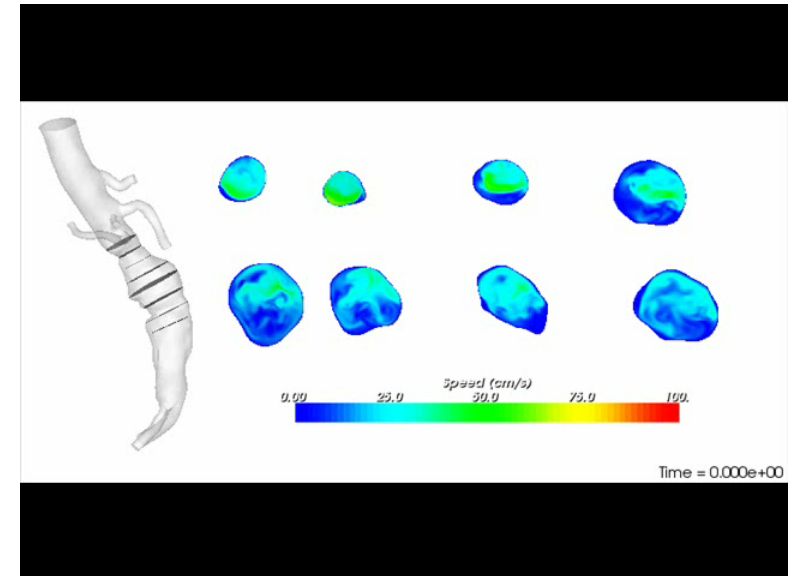
scale factor, $s_i = (t_{\text{base}} \times np_{\text{base}}) / (t_i \times np_i) - 1$ implies perfect scaling

Cores (avg. elems./core)	Cray XT3 PSC		Sun AMD TACC		IBM's BG/L RPI-CCNI	
	t (secs.)	scale factor	t (secs.)	scale factor	t (secs.)	scale factor
16 (96000) - base	390.84	1 (base)	425.96	1 (base)	2121.10	1 (base)
32 (48000)	190.63	1.03	208.73	1.02	1052.42	1.01
64 (24000)	89.57	1.09	98.10	1.09	528.62	1.00
128 (12000)	46.08	1.06	50.05	1.06	265.37	1.00
256 (6000)	24.49	1.00	27.70	0.96	132.83	1.00
512 (3000)	13.28	0.92	14.81	0.90	67.35	0.98
1024 (1500)	7.97	0.77	9.63	0.69	33.70	0.98
2048 (750)	-	-	-	-	17.13	0.97
4096 (375)	-	-	-	-	9.09	0.91
8192 (187)	-	-	-	-	5.00	0.83



Parallel Implicit Flow Solver – Incompressible Abdominal Aorta Aneurysm(AAA) 105 Million Elements

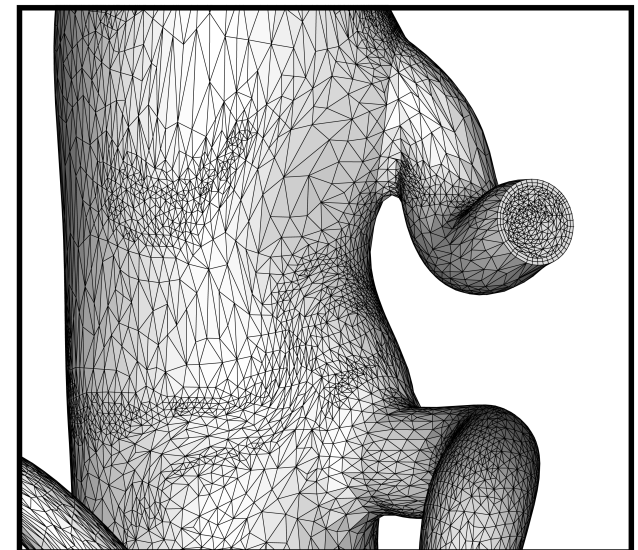
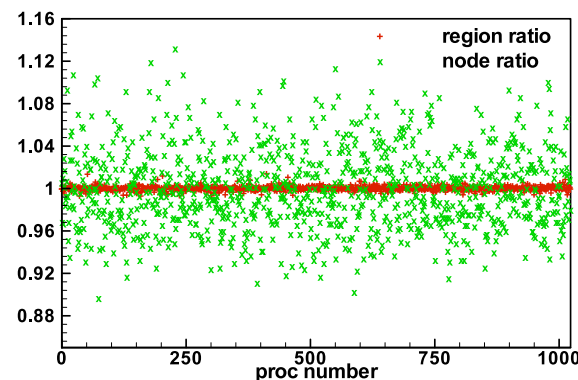
Cores (avg. elems./core)	IBM BG/L RPI-CCNI	
	t (secs.)	scale factor
512 (204800)	2119.7	1 (base)
1024 (102400)	1052.4	1.01
2048 (51200)	529.1	1.00
4096 (25600)	267.0	0.99
8192 (12800)	130.5	1.02
16384 (6400)	64.5	1.03
32768 (3200)	35.6	0.93



32K parts show modest degradation due to 15% node imbalance
(with only about 600 mesh-nodes/part)

$$\text{Rgn./elem. ratio}_i = \text{rgns}_i / \text{avg_rgns}$$

$$\text{Node ratio}_i = \text{nodes}_i / \text{avg_nodes}$$

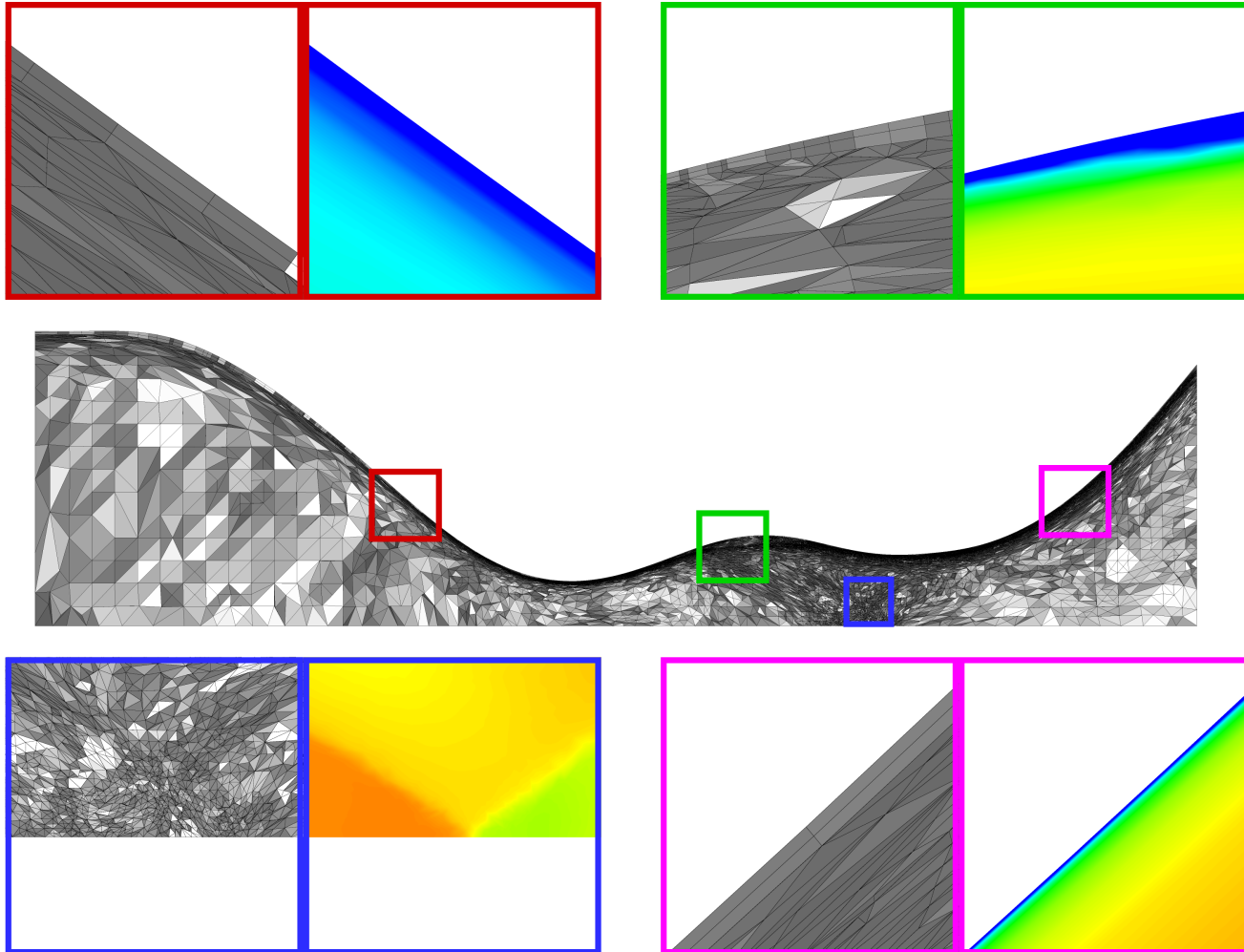


AAA Adapted to 10^9 Elements: Scaling on BG/P: Rigid Wall

#of cores	Rgn imb	Vtx imb	Time (s)	Scaling
32k	1.72%	8.11%	112.43	0.987
128k	5.49%	17.85%	31.35	0.885

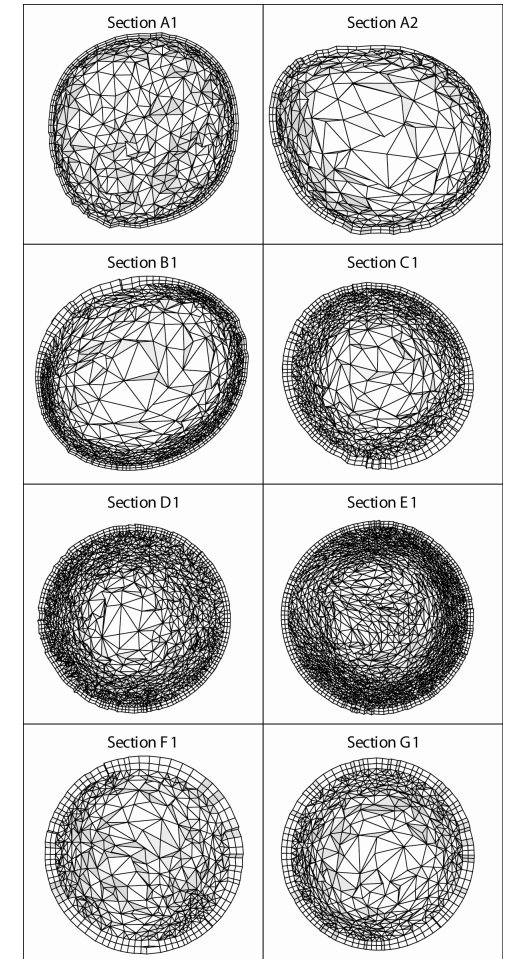
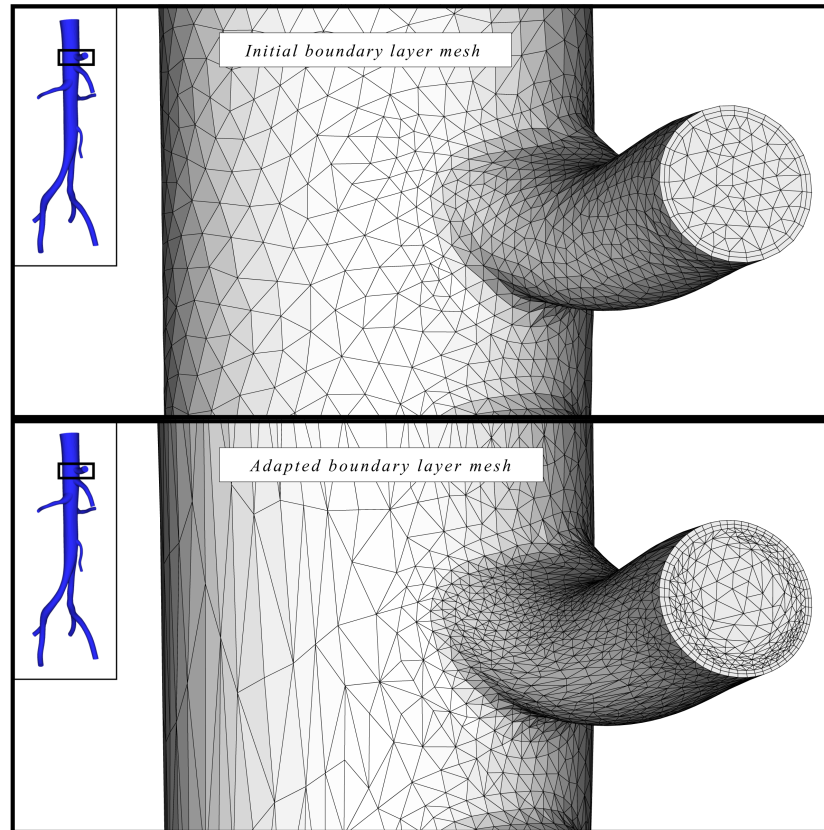
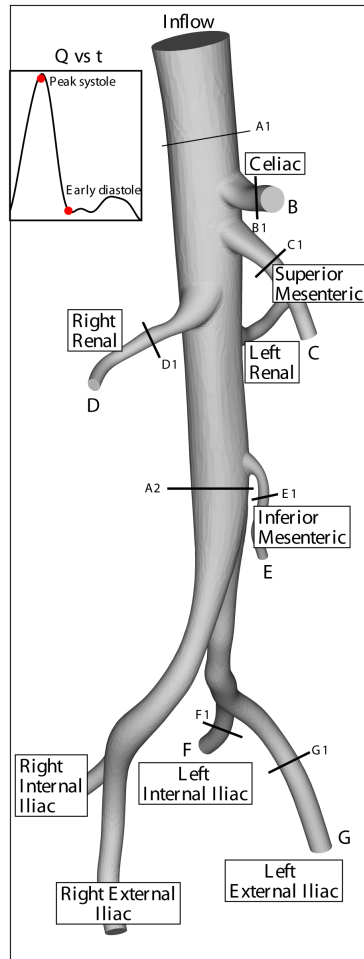
- **Billion** element cardiovascular **adapted** mesh on Kraken-NICS
 - Initial mesh: 128M regions on 512 parts
 - Repartitioned to 1024 parts and adapted to 1B regions in 2.5 min
 - Preprocessed PHASTA files on 1024 nodes in 3 minutes
 - All times include IO
- **Billion** element **adapted** mesh on **16K** cores of BG/L

Applications (Nozzle)



Zooms of clip plane of **adapted** mesh with Mach number

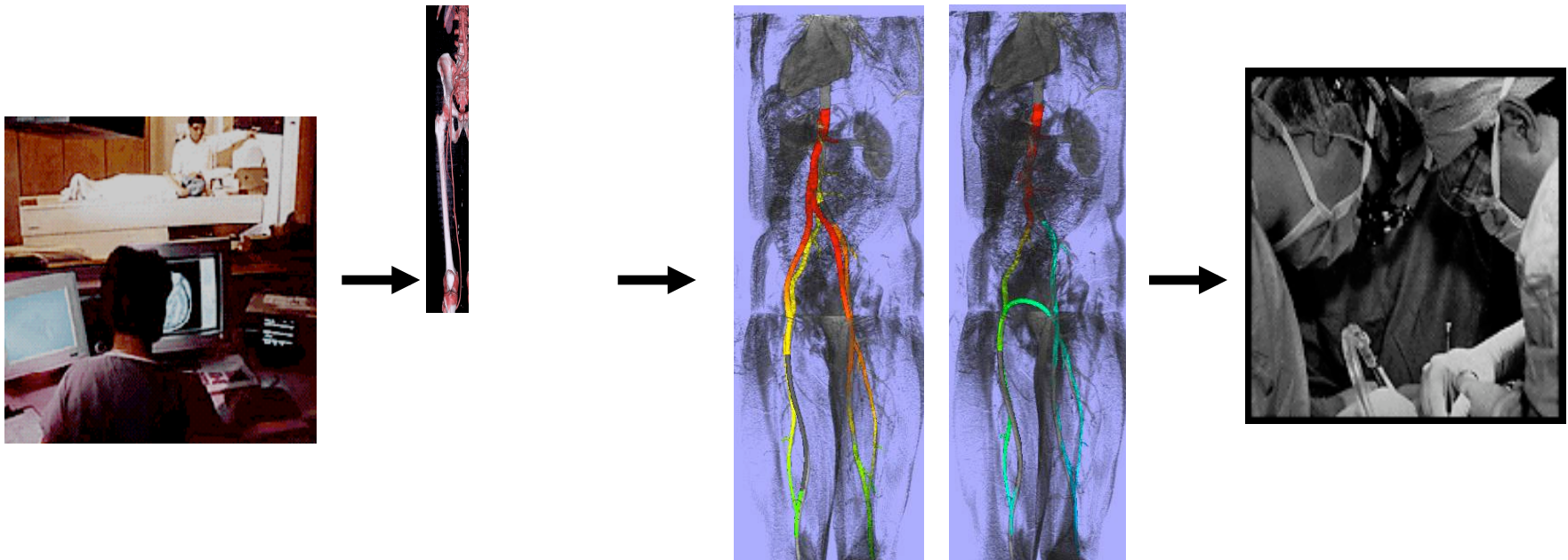
Healthy Human Abdominal Aorta



Petascale Adaptive CFD

- PetaApps Components
 - CFD Solver PHASTA
 - Adaptivity
 - Petascale Performance Simulation
 - Fault Recovery
 - **Demonstration Apps**
 - Two-phase Flow-(level set method)
 - Flow Control
 - Cardiovascular Flow

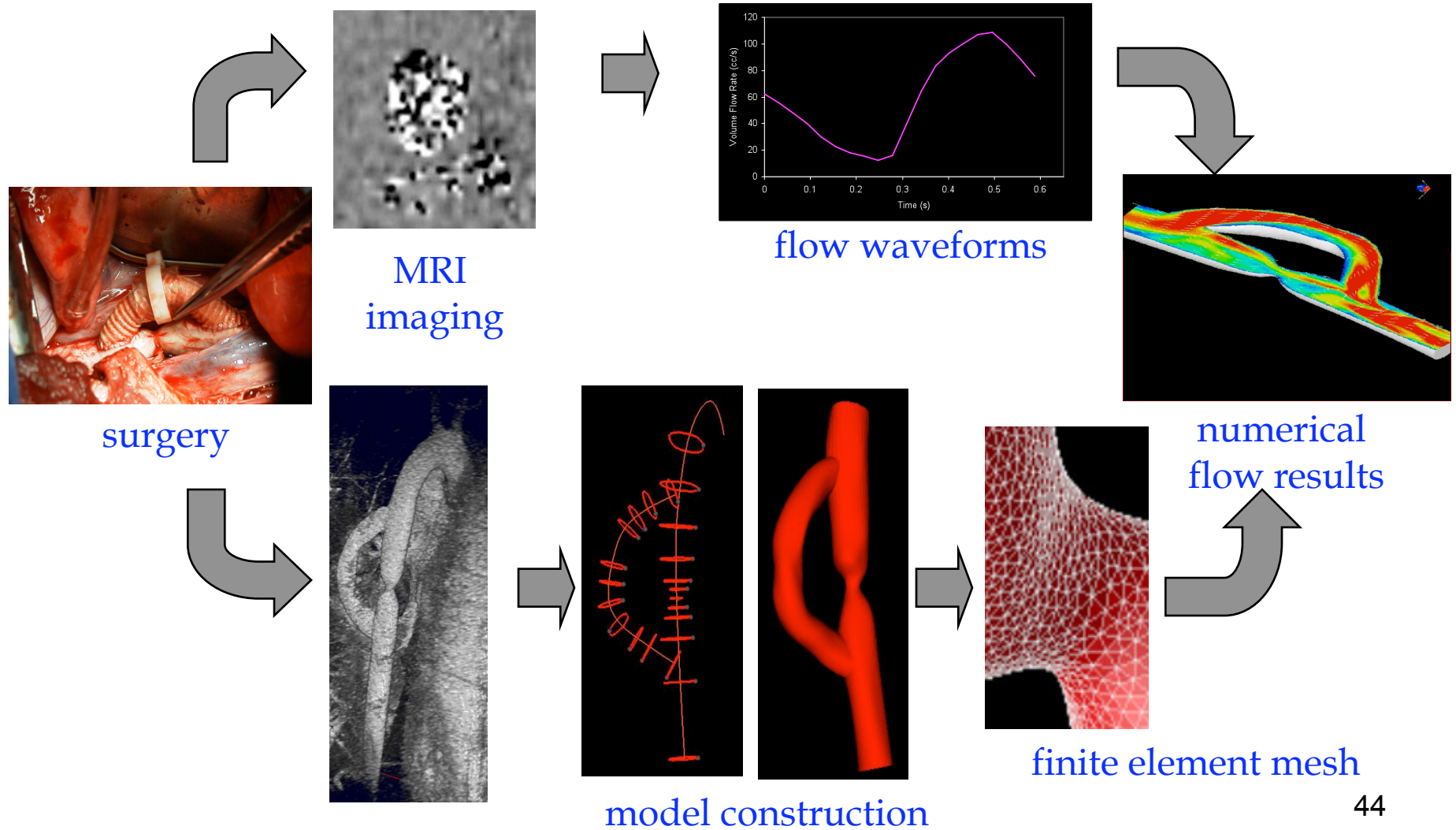
Simulation-Based Medical Planning w. Taylor



*Patient-specific models
constructed from diagnostic
imaging data*

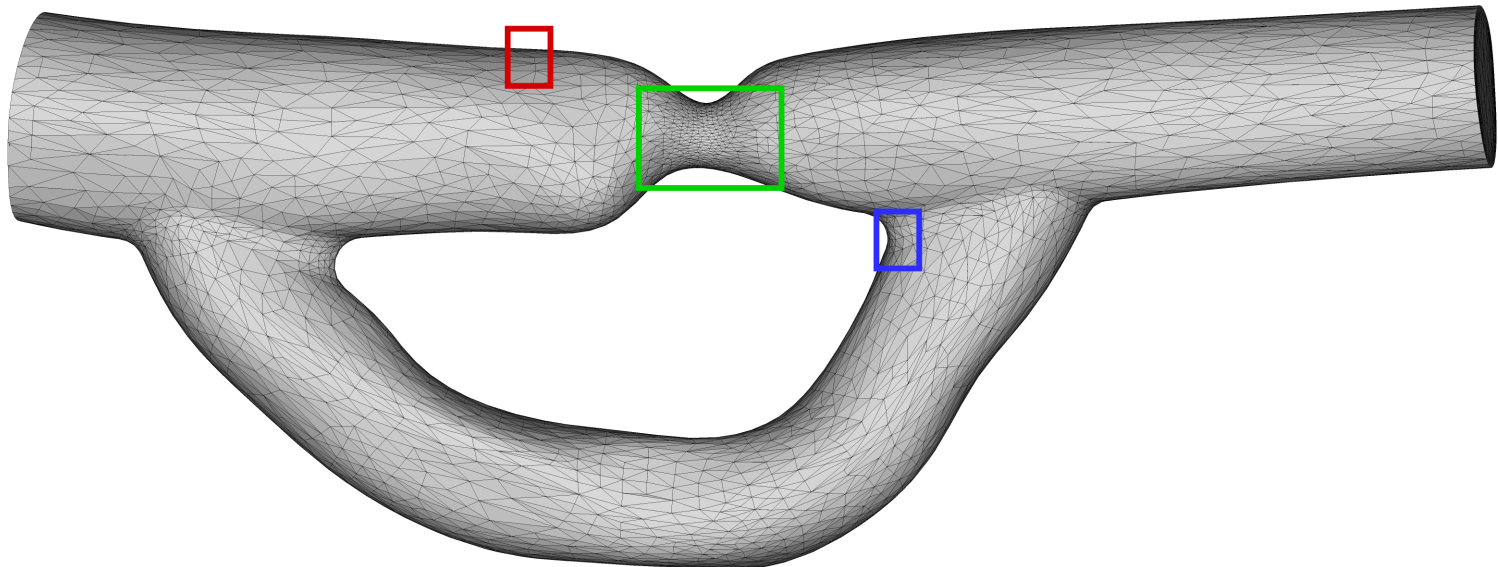
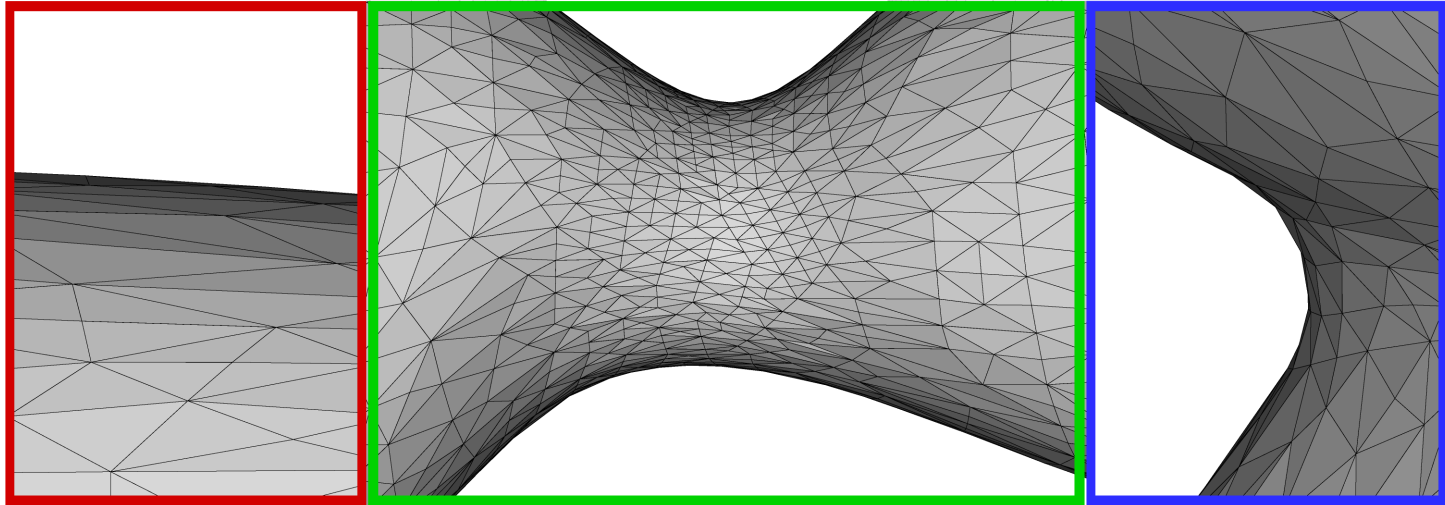
*Computer simulations
of blood flow to
evaluate alternate
treatments*

Generating Numerical Flow Solutions



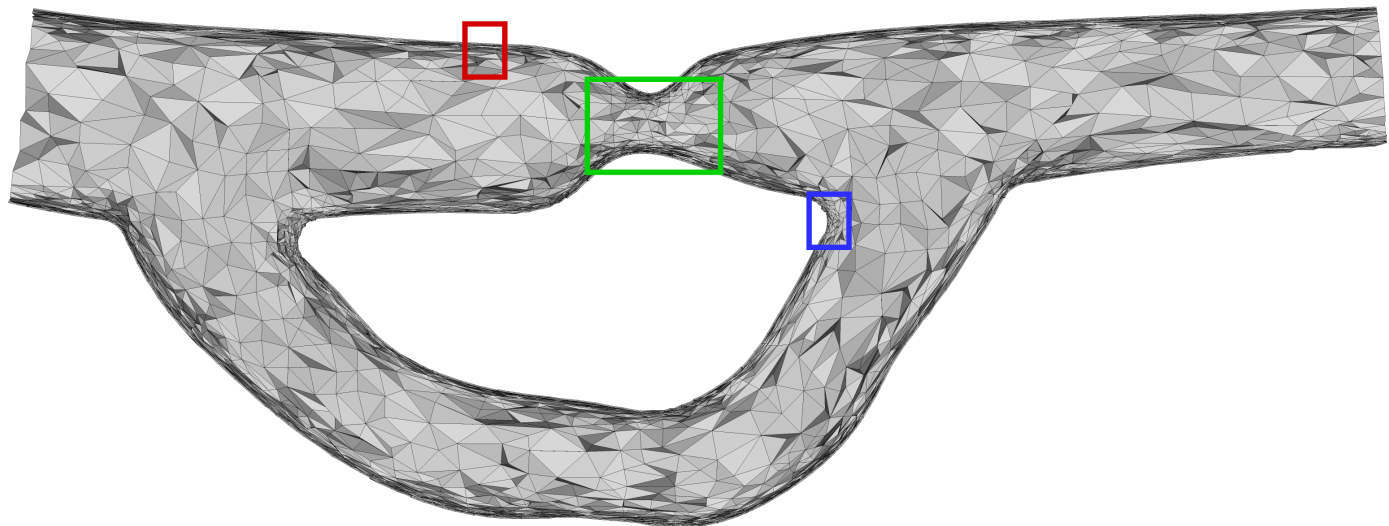
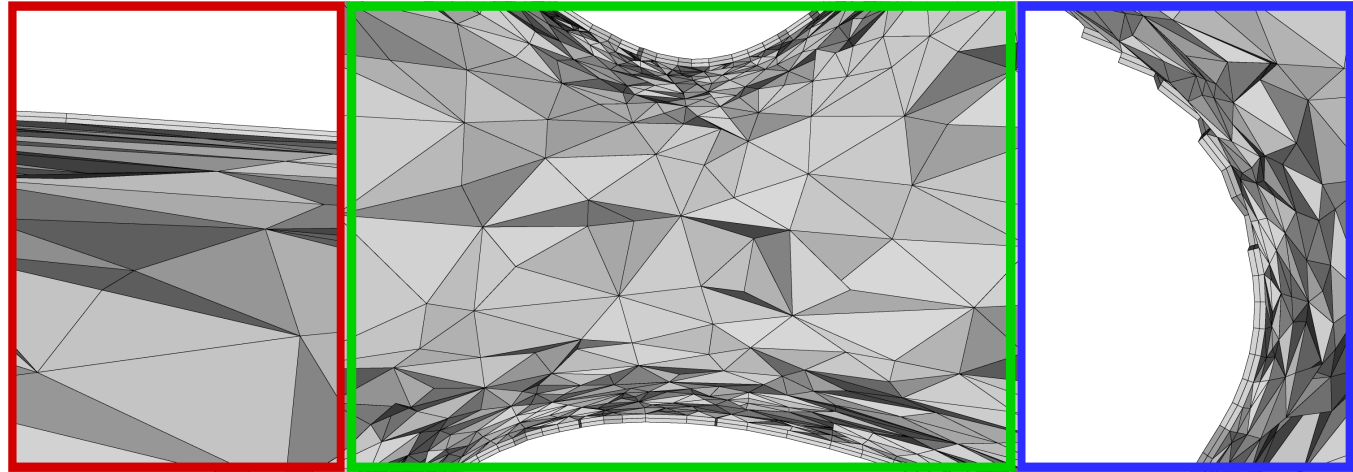
Surface Anisotropy

Surface of **adapted** mesh for porcine aorta



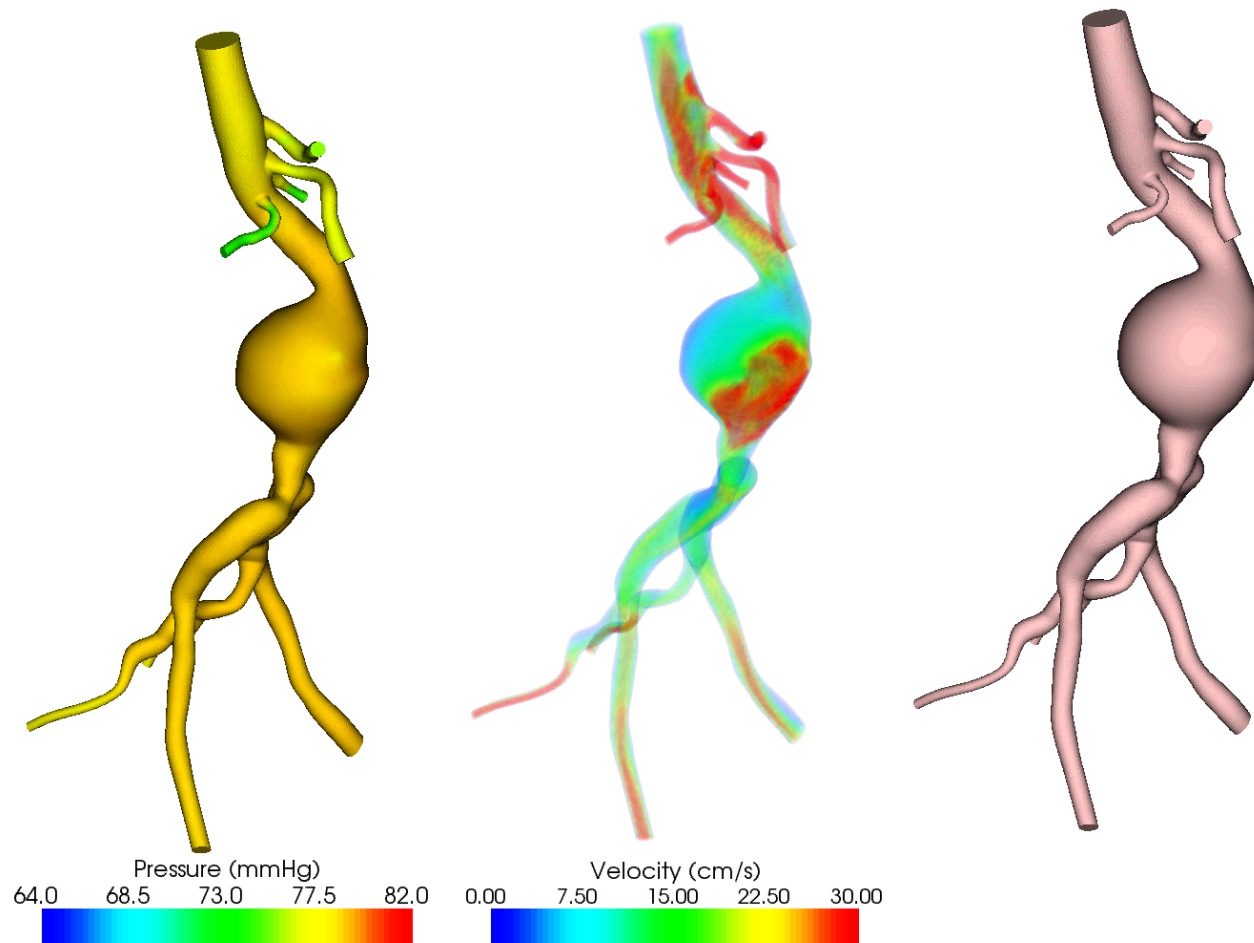
Interior Anisotropy

Clip plane of **adapted** mesh for porcine aorta



Wall Deformation (Figueroa)

- Fully coupled membrane model requires no mesh motion to capture vessel wall wave propagation at very small additional cost.



Scalability of CMM FSI

RigidWall

n core	eqn. form	solve	tot
16384	95.2	126.83	222.03
32768	47.56	64.87	112.43
65536	23.94	33.15	57.09
131072	12.48	18.86	31.35

DeformingWall

n core	eqn. form	solve	tot
16384	99.9	127.4	227.3
32768	49.9	64.9	114.8
65536	25.7	33.2	58.95
131072	13.42	18.7	32.12

- Time (sec)

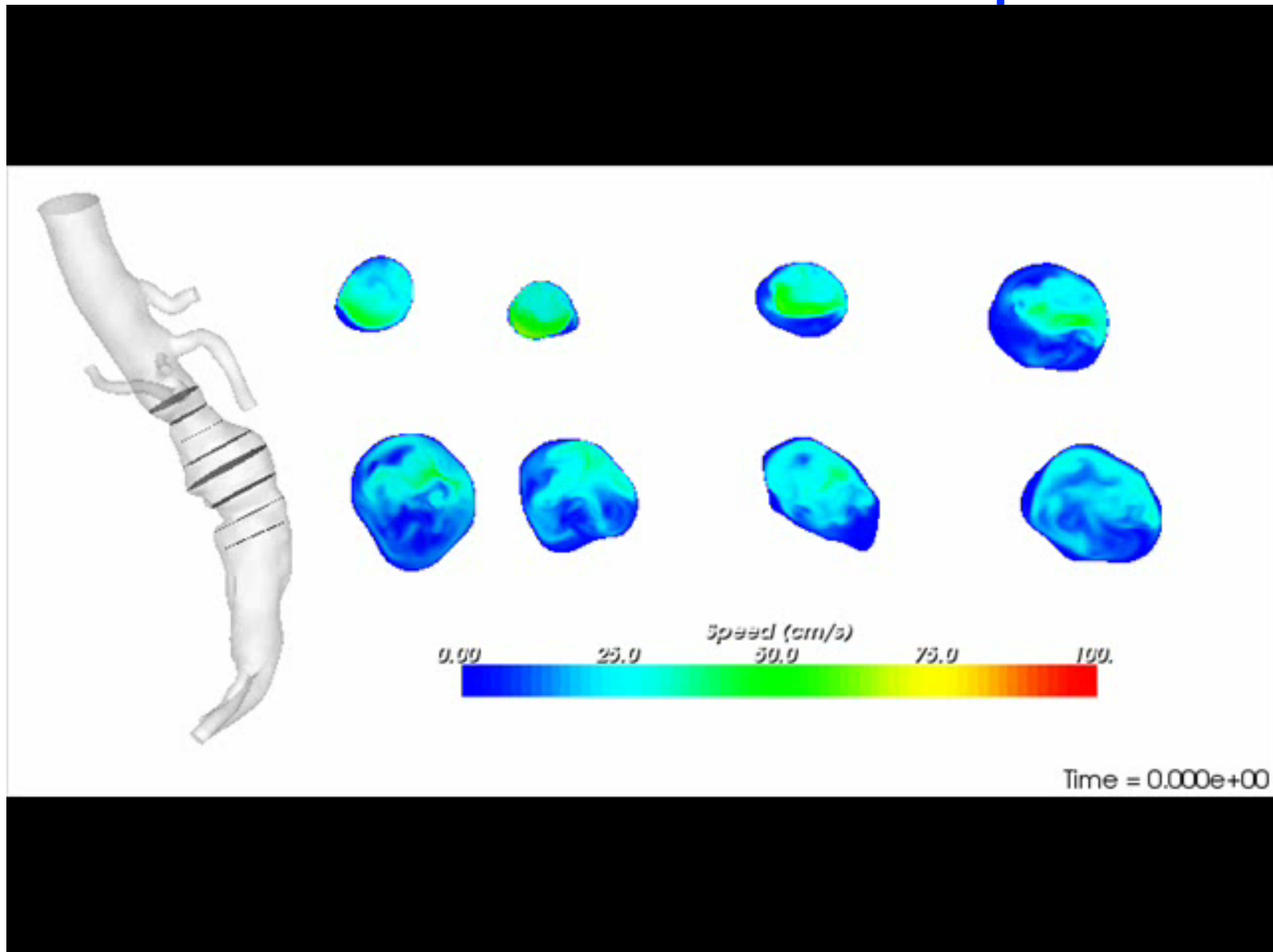
- Scaling

n core	S_e	S_s	S_t
16384	1.00	1.00	1.00
32768	1.00	0.98	0.99
65536	0.99	0.96	0.97
131072	0.95	0.84	0.89

n core	S_e	S_s	S_t
16384	1.00	1.00	1.00
32768	1.00	0.98	0.99
65536	0.973	0.96	0.96
131072	0.931	0.85	0.89

Slight degradation due to boundary element imbalance.

Transitional Flow Adapt 2



Biomedical Simulation: Scientific/ Engineering Value

- Patient-specific cardiovascular models offer physicians and clinical researchers a tool to understand flow in existing or planned (surgically modified) vasculature
- May also prove useful in understanding disease progression (aneurysm, stenosis, angiogenesis)
- Wall interactions (mechanical, physiological, and combinations) are complicated but very important.
- Early results suggest patient-specific geometric variability causes very large flow variation.
- Extension of modeling capability for human airways is underway (2 NIH grants pending).

Collaborations

- Research success is product of collaboration
- Maintaining existing, and growing new collaborations are vital to success at CUB
- Obvious areas discussed already include:
 - Fluids modeling and simulation (multiphase, turbulence)
 - Controls: fluids, structures, and combination
 - Fluids structure interaction
 - Biological flows (including reduced/low gravity effects)
 - Massively parallel simulation (not just fluids)
- Open to new areas as well. 1/2 hour chat with:
 - R.T. Lahey spawned multiphase simulation
 - C.A. Taylor spawned cardiovascular simulation
 - M. Amitay spawned flow control simulation

Teaching/Advisement

- Teaching experience in broad array of classes (statics, thermal fluids, aerodynamics, graduate fluids, FEM, CFD, turbulence).
- Graduate student's research focused on CFD but with variable weights on three foundations:
 - Physics/engineering of fluid dynamics
 - Math discretization methods, boundary conditions
 - Computer science: serial and parallel performance
- At least one category must be very strong, other two adequate competency (and willing to grow).
- Some topics, like turbulence modeling require significant strength in two.

- Thanks

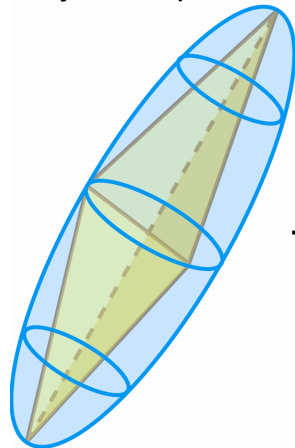
Automatic Anisotropic Adaptive Simulations

- Key components for adaptive mesh-based flow simulations:
 - Directional error indicators: determine error distribution (qualitatively)
solution field's second derivatives in form of Hessian matrix: $H = R\Lambda R^T$
(where, R is matrix of eigenvectors p_k and Λ is diagonal matrix of eigenvalues λ_k)
 - Mesh size field: specify anisotropic mesh resolution by using metric tensors
equi-distribution of error leads to: $h_k^2 |\lambda_k| = \varepsilon$
(where, h_k is desired size along p_k and ε is relative tolerance value controlled by user)
 - Mesh modifications: alter mesh resolution while maintaining favorable attributes
apply local mesh modifications that preserve the favorable attributes
(like edge collapse, split and swap)

Error Indicators and Mesh Size Field

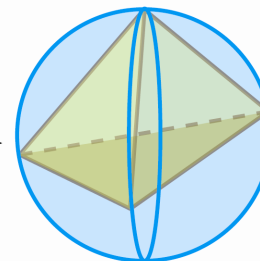
- Translate directional error indicators into mesh size (resolution) field by using mesh metric tensors at each mesh node:
 - Construct mesh size field
attempt uniform distribution of local errors to user controlled level (ϵ)
 - Determine mesh metric tensor at each mesh node
evaluate symmetric positive definite second-order tensor: $M = R\Lambda R^T$, where $\Lambda = \Lambda/\epsilon$

Physical space : $X^T M X = 1$



— Transformation —→

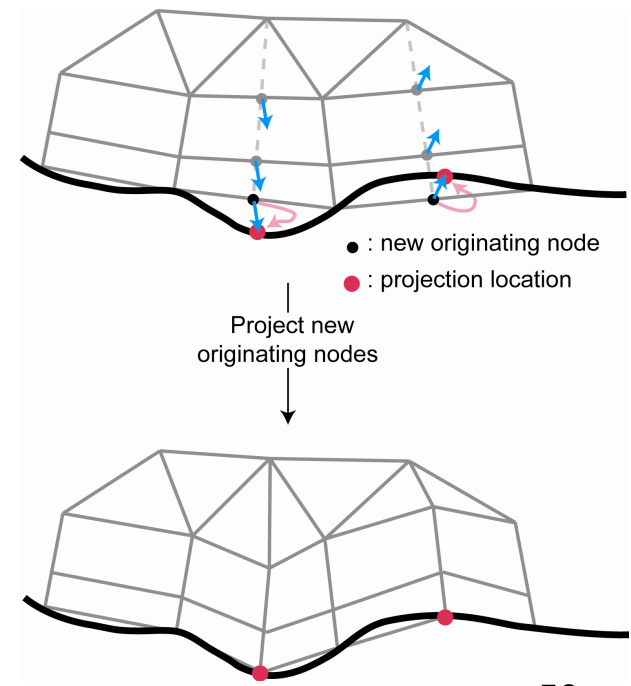
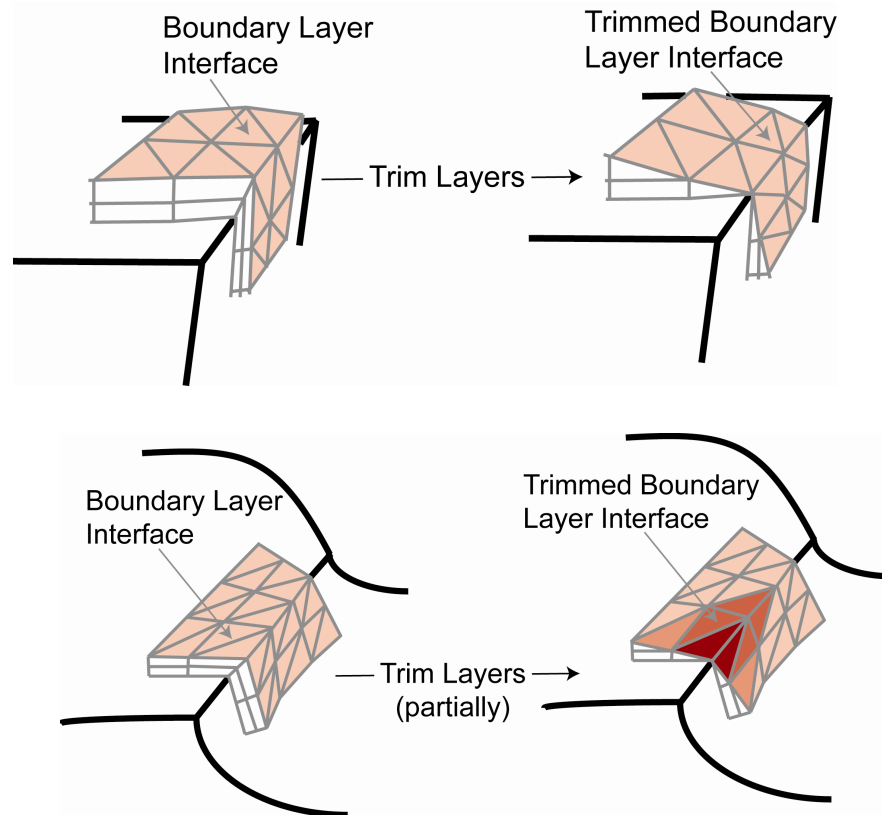
Metric space : $x^T x = 1$



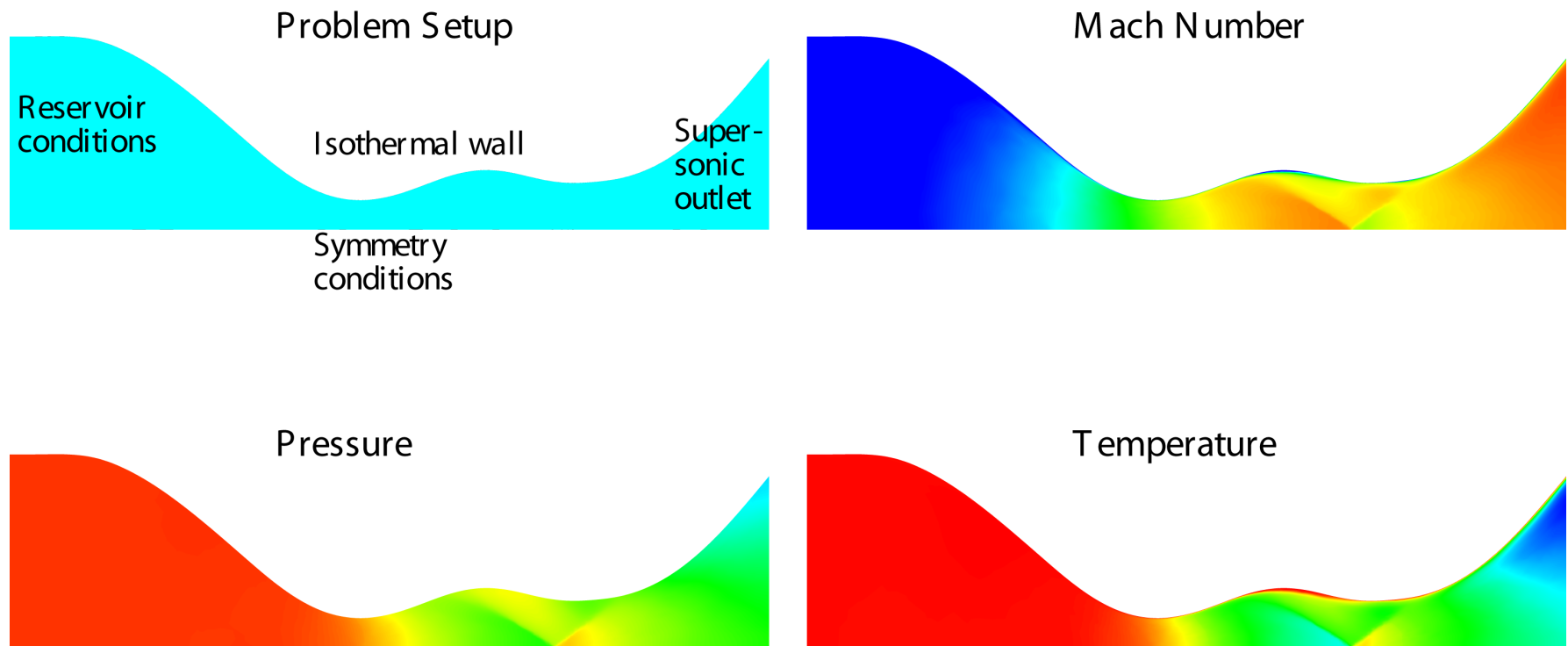
- Goal is to create regular elements with unit sides in the metric space
 $\langle \mathbf{e}, M\mathbf{e} \rangle = 1$, where \mathbf{e} is vector associated with mesh edge

Dealing with Realistic Geometries

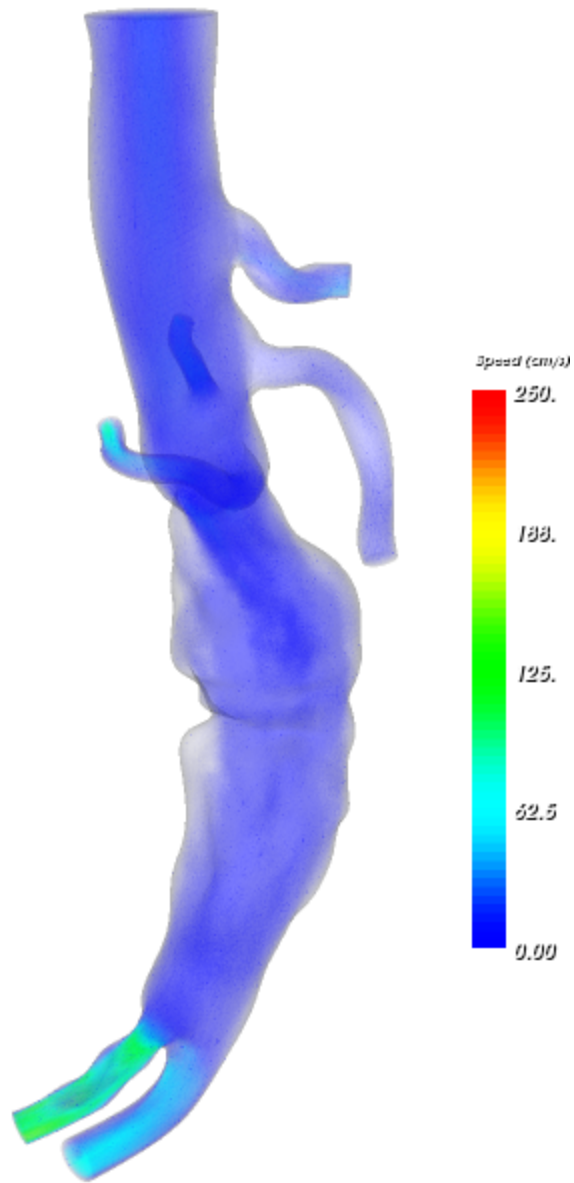
- Trim layers at corners to avoid poor quality elements (*transition elements with mixed topologies*) (O. Sahni).
- Project newly create nodes at curved boundary onto the solid model surface to improve geometric approximation.



Demonstration (Nozzle)



Transitional Flow

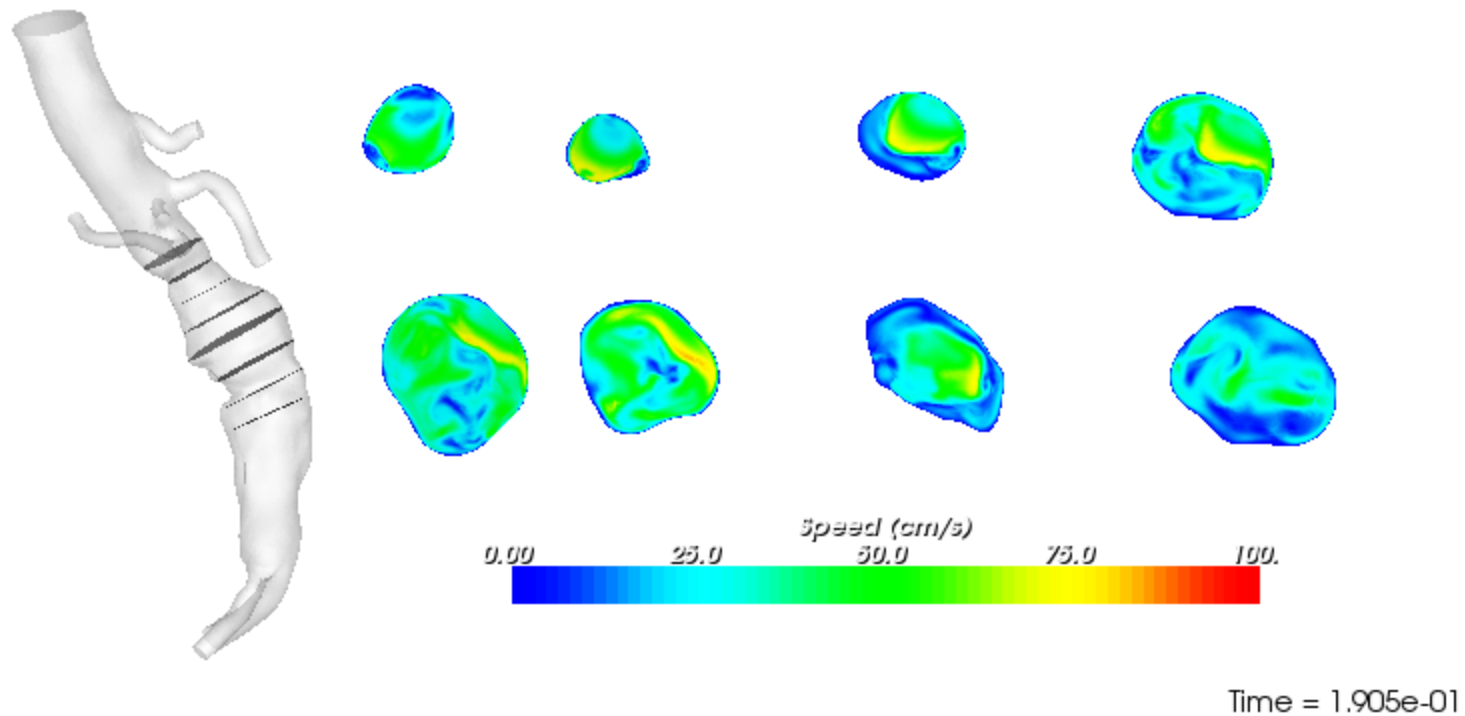


Time = 0.000e+00

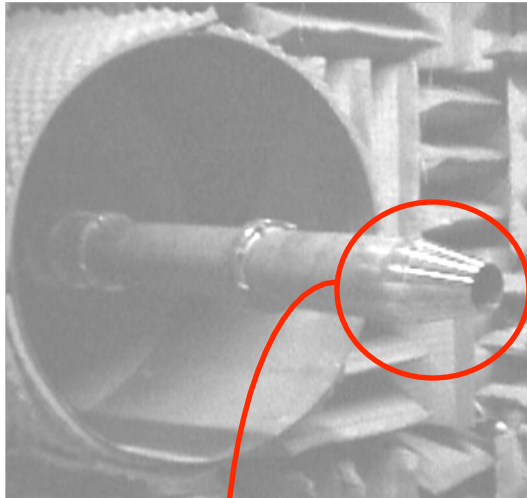


Slices of Transitional Region

- Adaptation 1



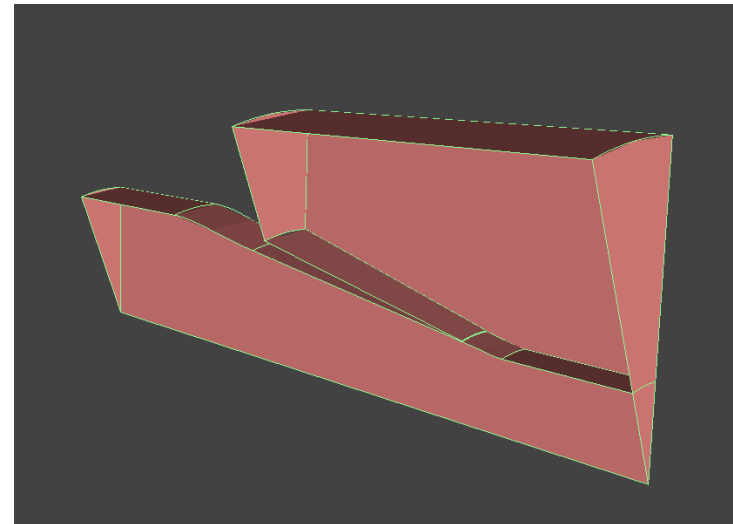
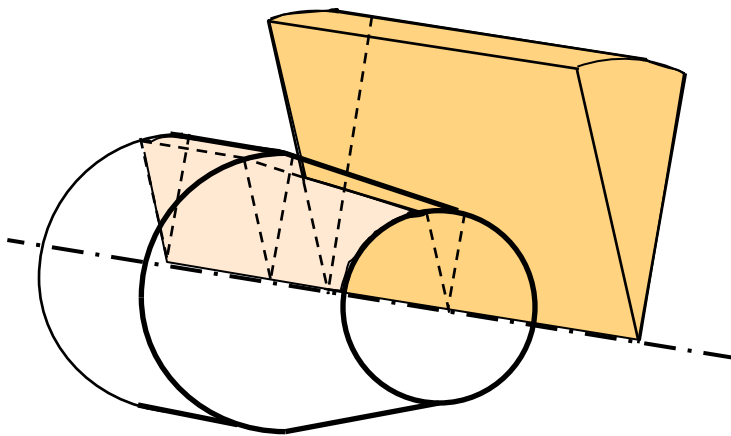
Large Eddy Simulation of Jet Flow with Complex geometry



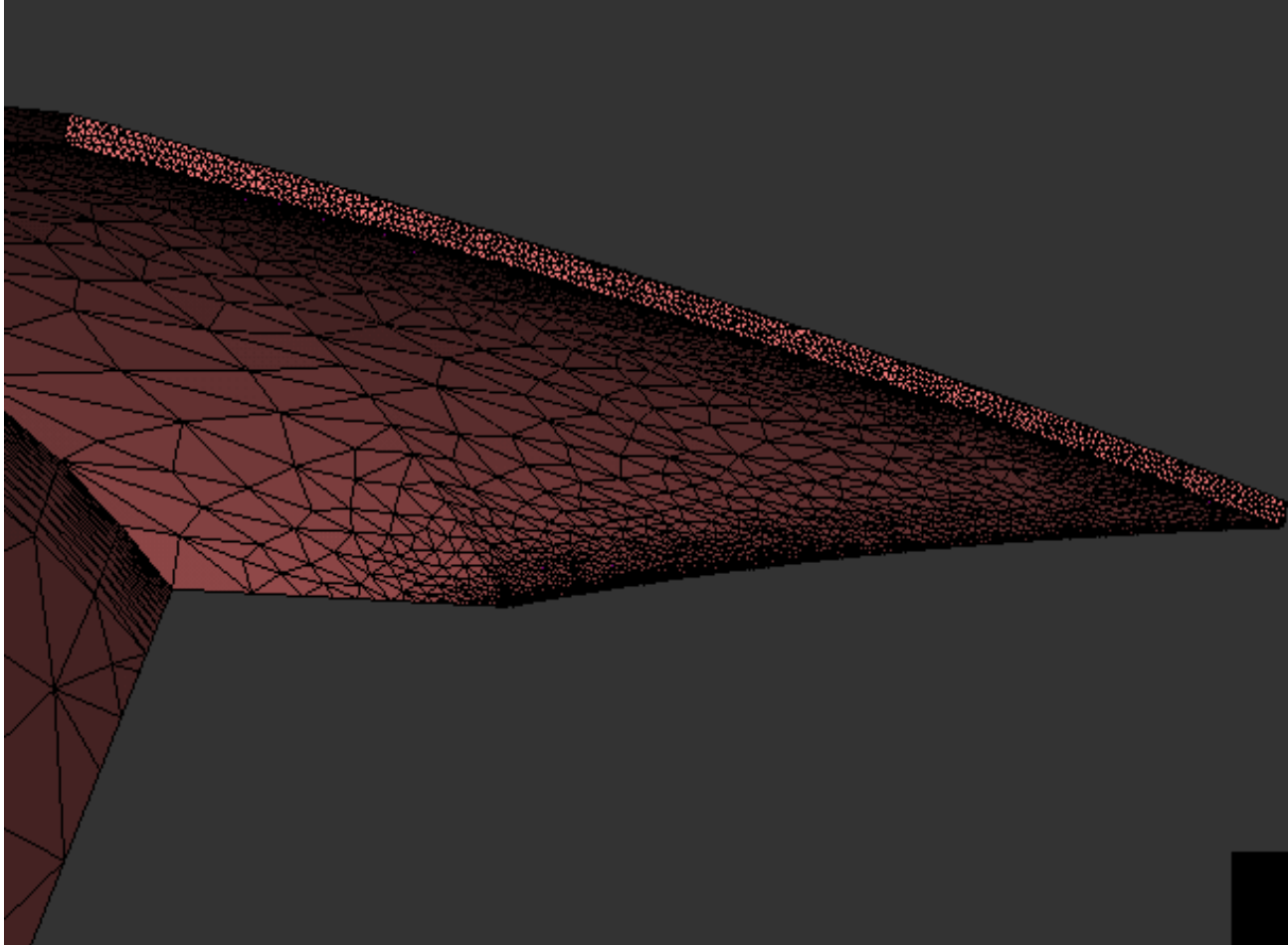
- initial problem: ART single-stream cold jet at $Ma = 0.6$ and $Re_D = 10^6$

- full problem too costly \rightarrow simulate a representative sector of the flow with a limited streamwise extent

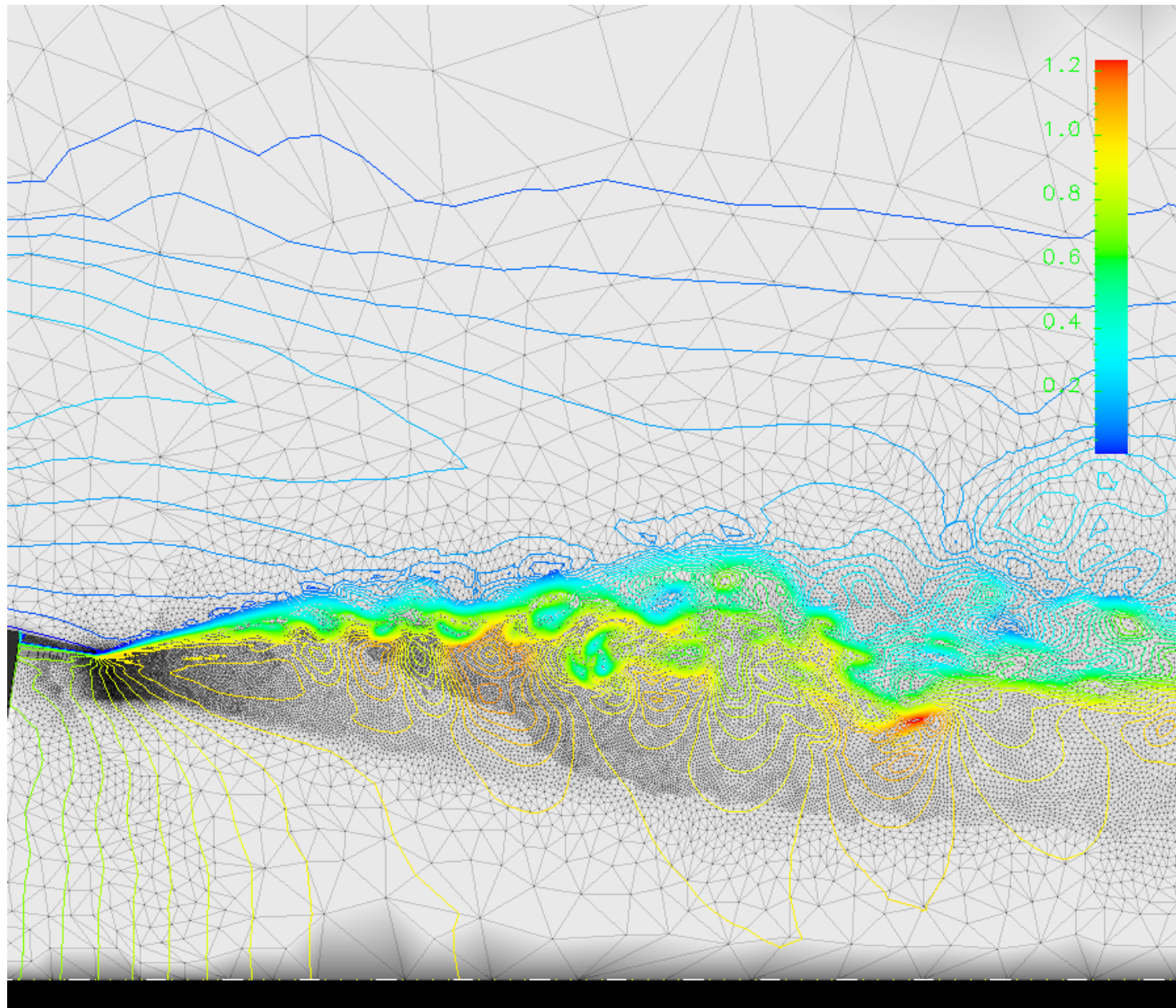
- evolution: add complexity (tabs, core flow), study effects of compressibility



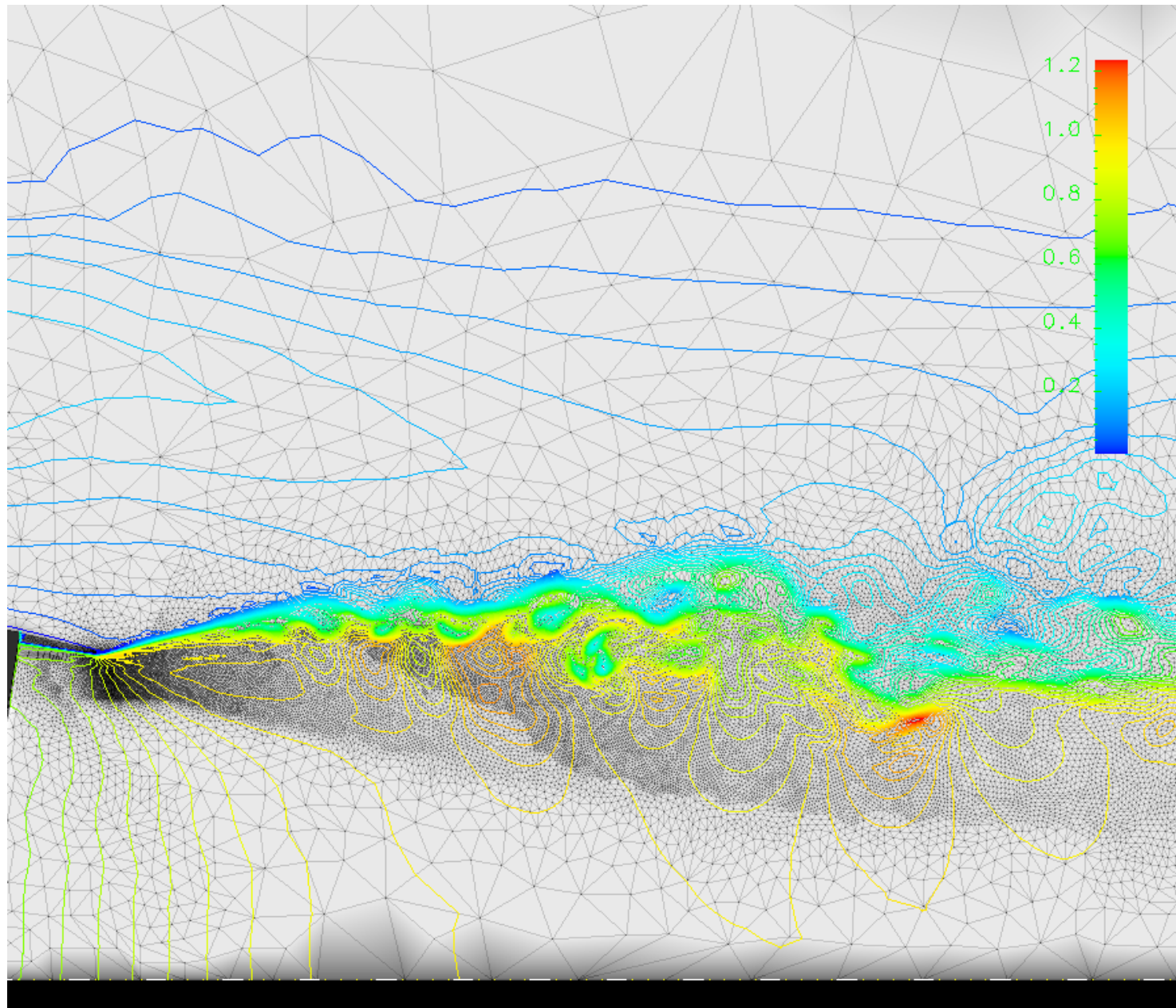
LES Grid (tab surface)



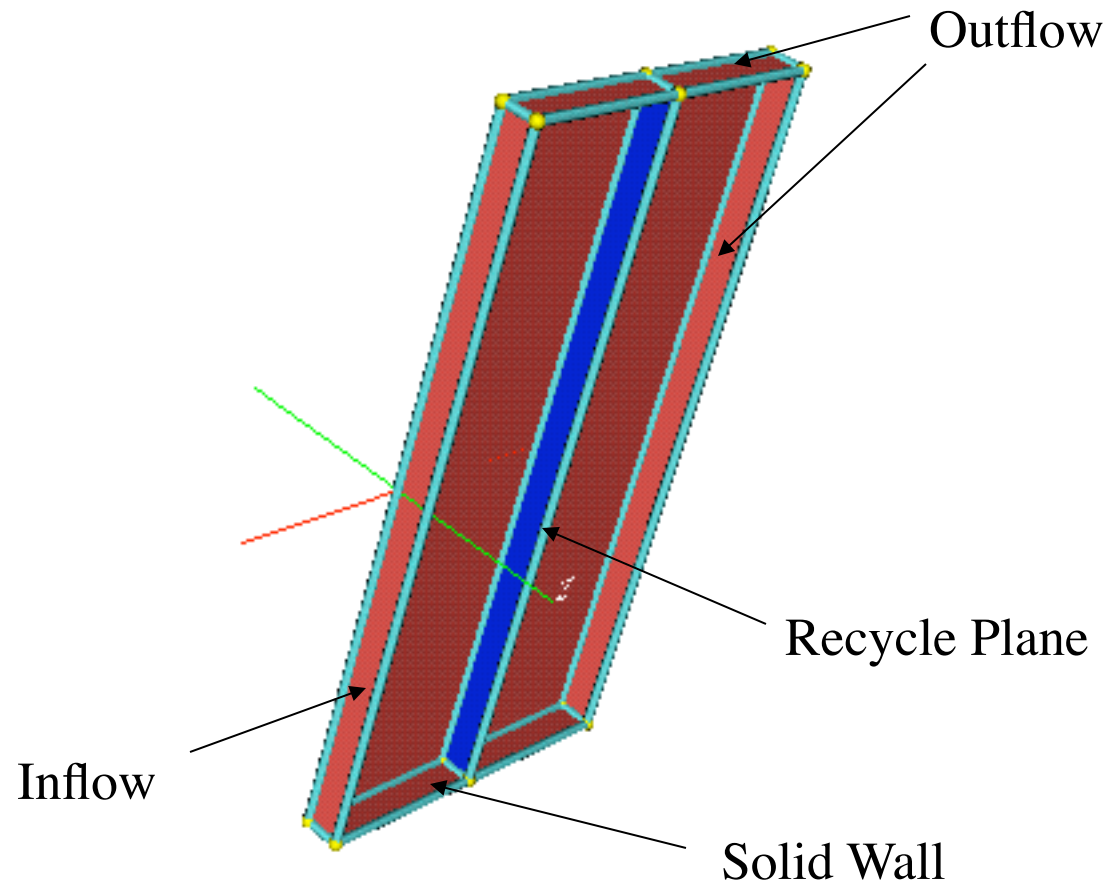
Axial Velocity on Refined Grid on the Root Plane



Axial Velocity on Refined Grid on the Root Plane



Hybrid Modeling: Boundary Layer Rescaling

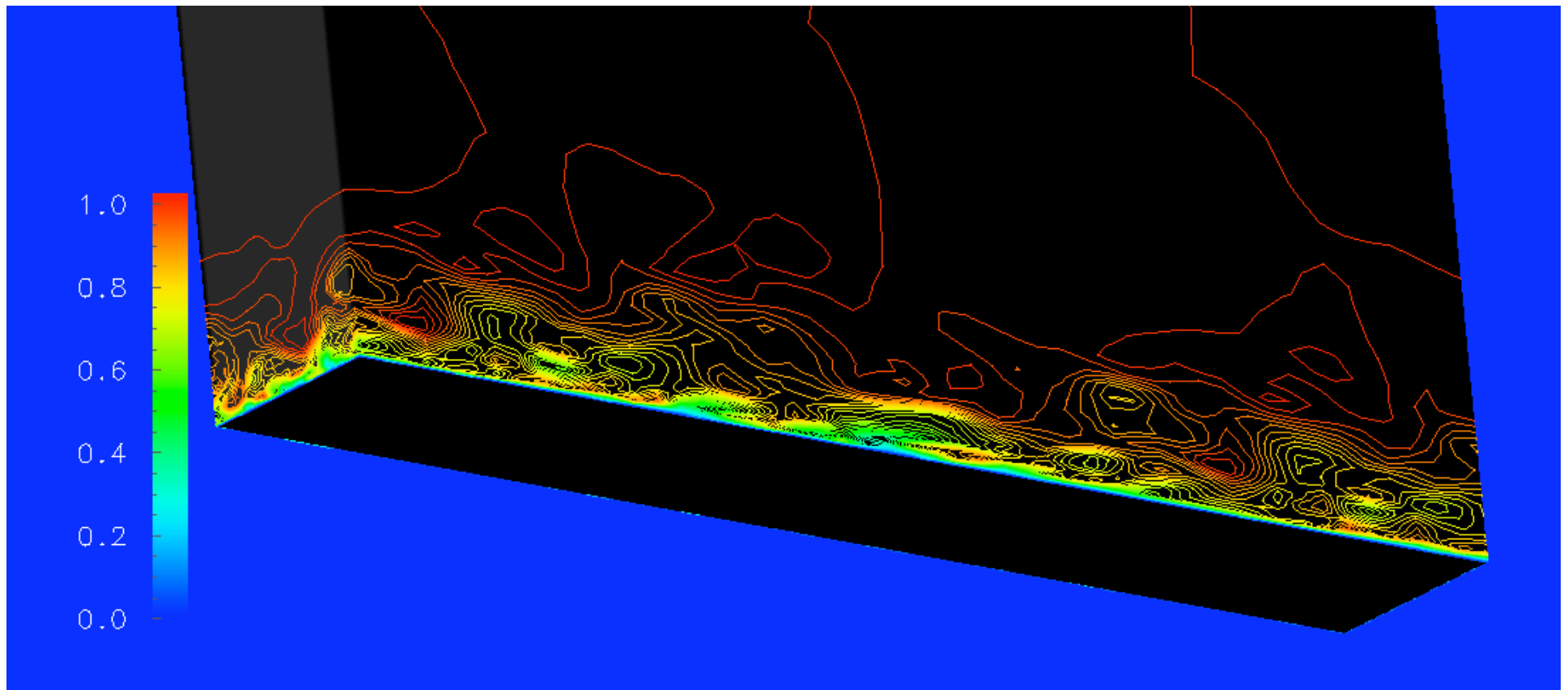


The velocity fluctuations are interpolated from the recycle plane (with appropriate scaling to reflect boundary layer growth and shear stress decay).

Recycled Turbulent Boundary Layer

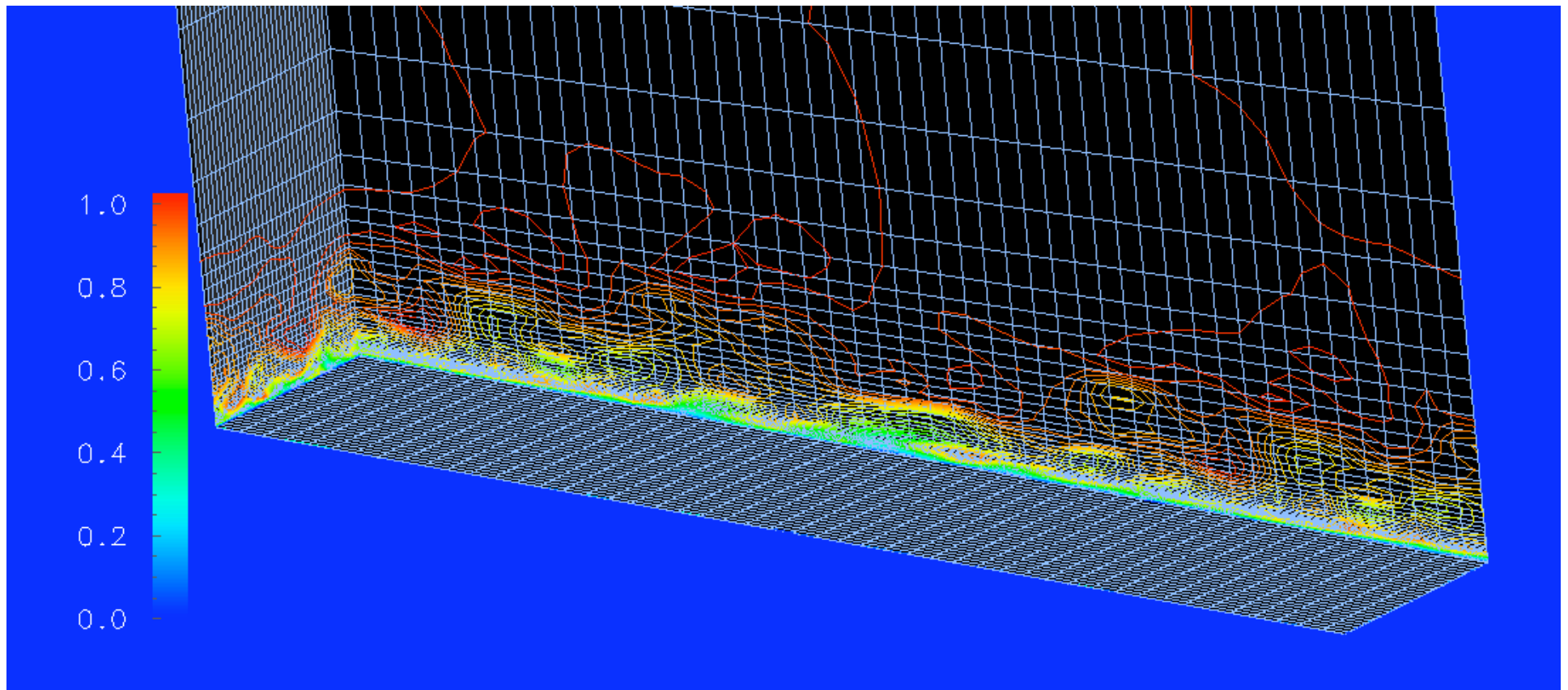
$$\text{Re}_\theta = 1400$$

(Mean velocity set to RANSS profile at inflow)



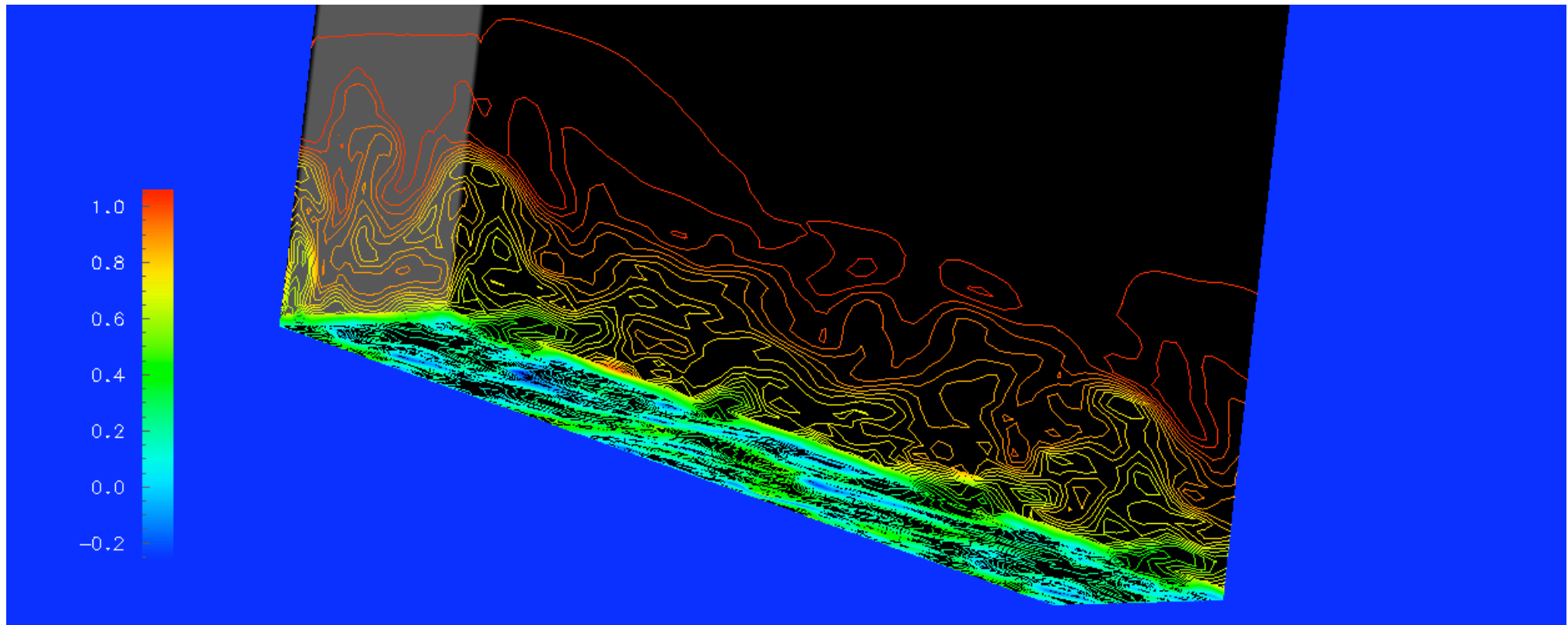
Turbulent Boundary Layer

$Re_{\theta} = 1400$ (Computational grid in wall resolved case)

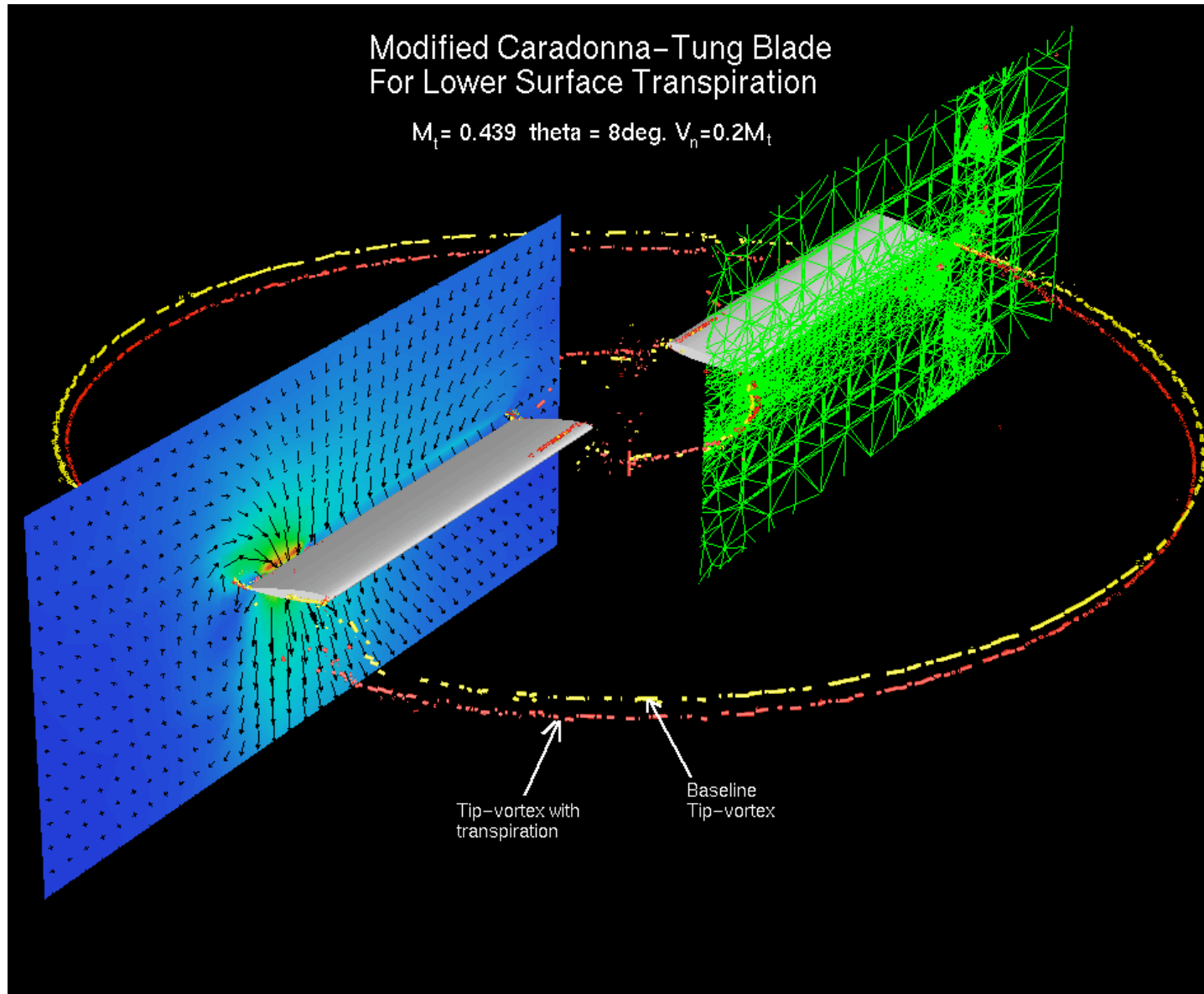


Turbulent Boundary Layer: Wall Model

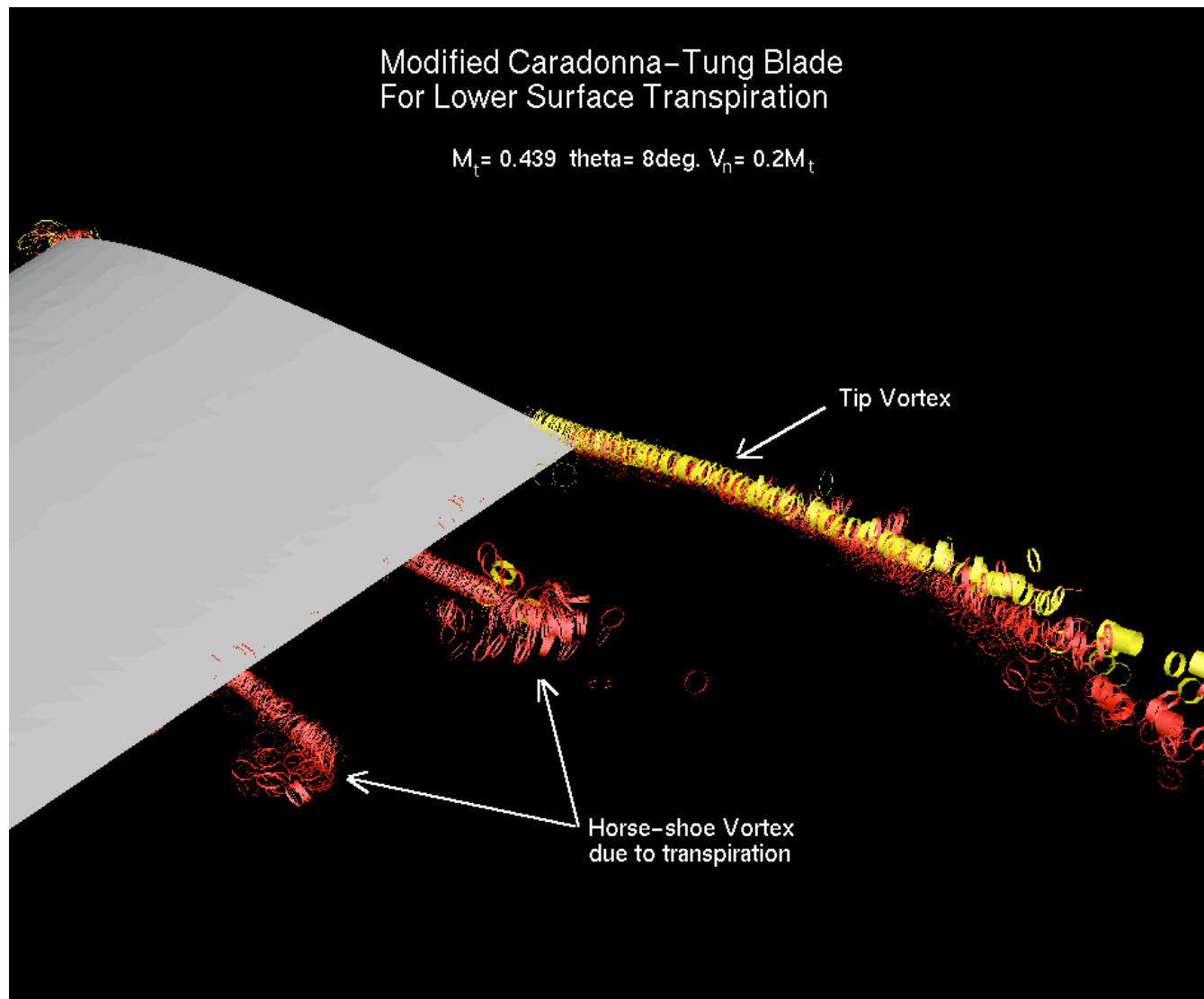
$$\text{Re}_{\theta} = 7100$$



Blade Vortex Interaction



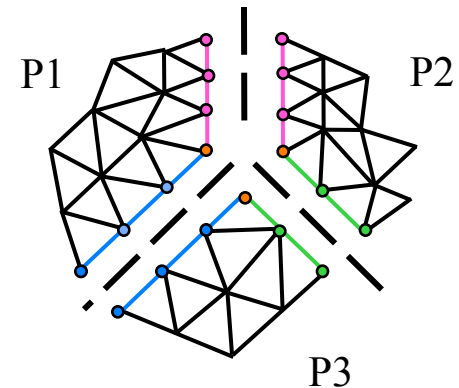
Blade Vortex: Flow Control



- Thank You

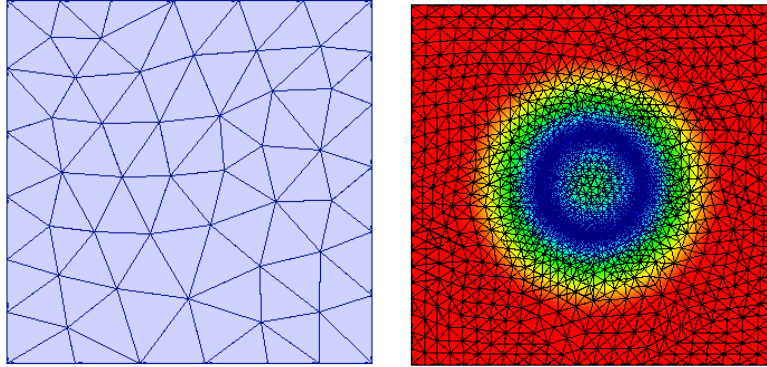
Flow Solver Parallel Paradigm

- Time-accurate, stabilized FEM flow solver
- Two types of work:
 - Equation formation
 - $O(40)$ peer-to-peer non/blocking comms
 - Overlapping comms with comp
 - Scales well on many machines
 - Implicit, iterative equation solution
 - Matrix assembled on processor ONLY
 - Each Krylov vector is:
 - $q=Ap$ (matrix-vector product)
 - Same peer-to-peer comm of q PLUS
 - Orthogonalize against prior vectors
 - REQUIRES NORMS \Rightarrow MPI_Allreduce
 - This sets up a cycle of global comms. separated by modest amount of work
 - Not currently able to overlap Comms
 - Even if work is balanced perfectly, OS jitter can imbalance it.
 - Imbalance WILL show up in MPI_Allreduce
 - Scales well on machines with low noise (like Blue Gene)



Parallel Mesh Adaptivity

- **Billion element adapted mesh on 16K cores of BG/L (with 512MB mem.):**



Magnified view of initial and adapted mesh
(zoom for 1/2 air-bubble, colored by mesh size-
field)

- Initial mesh: uniform, 17.2M mesh elems. (1K elems./core).
 - Adapted mesh: 160 air-bubbles, 1.06B mesh elems. (65K elems./core).
 - Multiple predictive load balance steps needed to make the adaptation possible.
- **Billion element cardiovascular adapted mesh on Kraken-NICS**
 - Initial mesh: 128M regions on 512 parts
 - Repartitioned to 1024 parts and adapted to 1B regions in 2.5 min
 - Preprocessed PHASTA files on 1024 nodes in 3 minutes
 - All times include IO
 - Only initial mesh uses global address space; once partitioned no more

Motivation: Adaptive, Implicit CFD

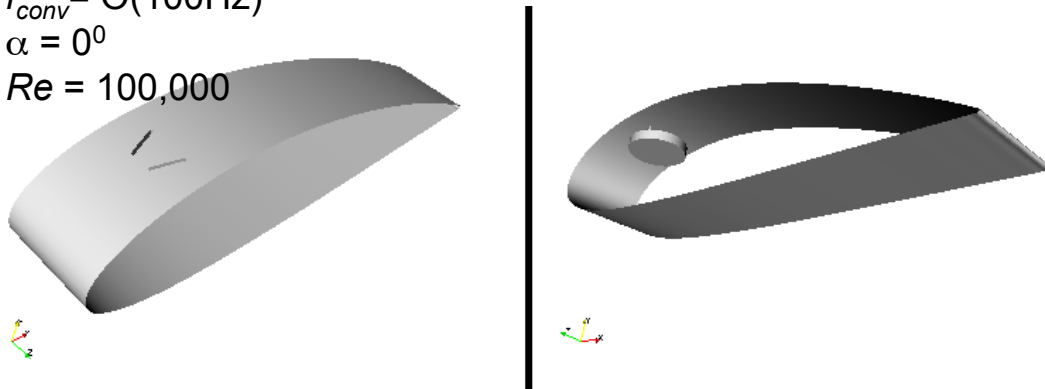
- Viscous flow in complex geometry:
 - Making a “good” initial mesh is often not possible
 - Explicit time integration is often stability bound
 - Physical length scales develop anisotropy $> 200 \times 50 \times 1$
 - Ratio of length scales easily exceeds 10^4
- Are there simpler alternatives?
 - Cartesian cut cell methods use 10^9 times more cells
 - Structured AMR could use 10^5 times more cells
 - Fourier spectral benchmark's are great but.....
- Anisotropic, adaptive, implicit finite element method is complex but worth it and CAN scale

Synthetic Jet Calibration in CFD

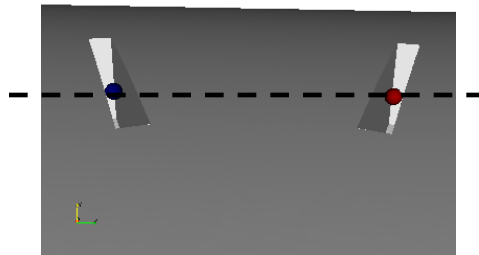
- Velocity profile (sinusoidal in time and parabolic in space) is prescribed at the diaphragm surface such that it matches with the experimental data (with no cross-flow) at probes near the jet exits:

One (first) pair of synthetic jets

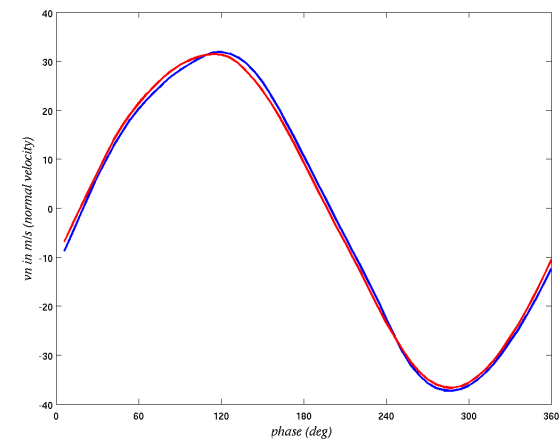
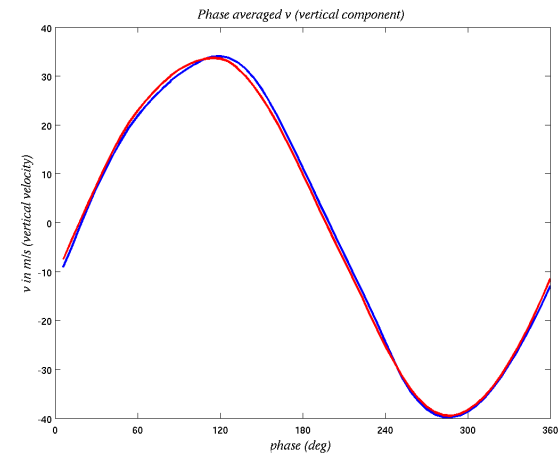
$$\begin{aligned} C_\mu &= 7.25 \times 10^{-3} \\ C_b &= 3.2 \\ f_{act} &= 2,300 \text{ Hz} \\ f_{conv} &= O(100 \text{ Hz}) \\ \alpha &= 0^\circ \\ Re &= 100,000 \end{aligned}$$



Probes near jet exits

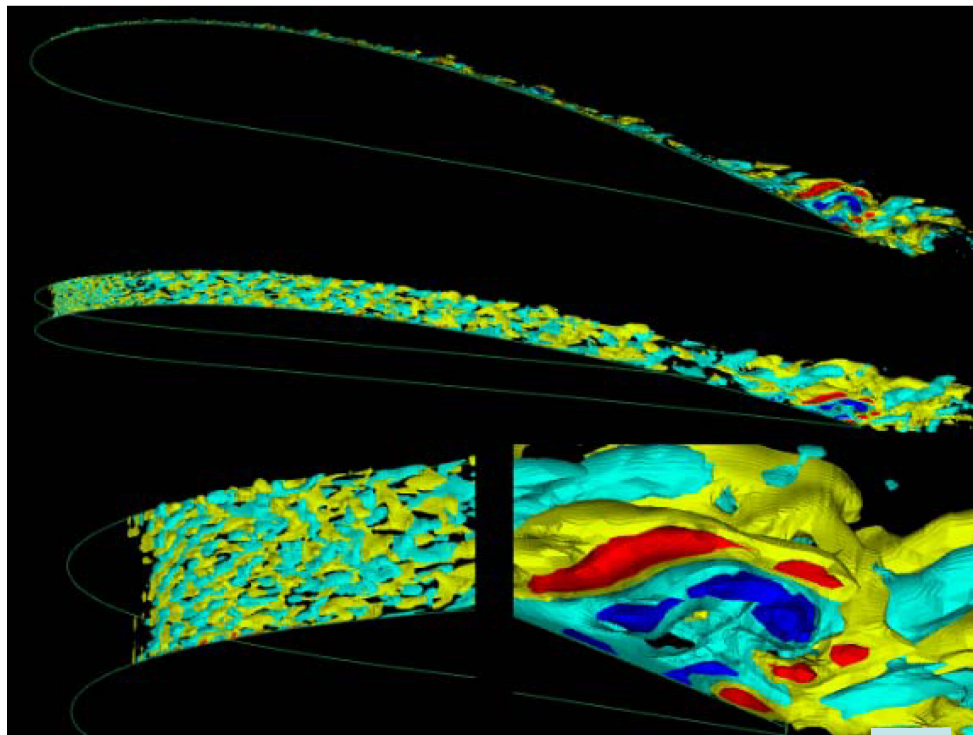


Phase-averaged (50 cycles) at two probes

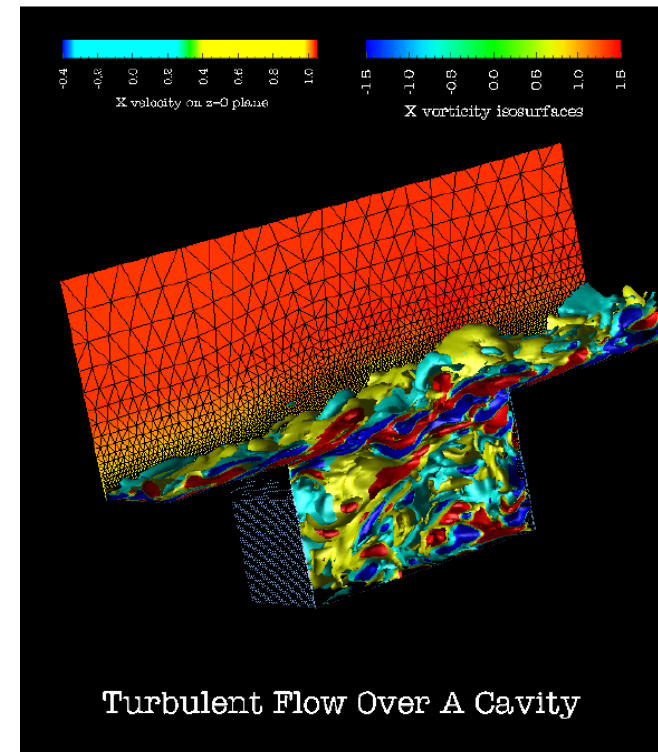


Flow Control: Motivation

- High lift airfoil (1996)



- Cavity (1998)



- Idea: with small ($<2\%$) precisely located and directed flow, create a major change/improvement to bulk flow.

Scalability of CMM FSI

RigidWall

DeformingWall

- Time (sec)

n core	eqn. form	solve	tot
16384	95.2	126.83	222.03
32768	47.56	64.87	112.43
65536	23.94	33.15	57.09
131072	12.48	18.86	31.35

n core	eqn. form	solve	tot
16384	99.9	127.4	227.3
32768	49.9	64.9	114.8
65536	25.7	33.2	58.95
131072	13.42	18.7	32.12

- Scaling

n core	S_e	S_s	S_t
16384	1.00	1.00	1.00
32768	1.00	0.98	0.99
65536	0.99	0.96	0.97
131072	0.95	0.84	0.89

n core	S_e	S_s	S_t
16384	1.00	1.00	1.00
32768	1.00	0.98	0.99
65536	0.973	0.96	0.96
131072	0.931	0.85	0.89

- Balance

n core	B_e	B_n
16384	1.022	1.07
32768	1.017	1.084
65536	1.024	1.117
131072	1.055	1.17

Slight degradation due to
Boundary element imbalance.